universität wien

MASTERARBEIT / MASTER'S THESIS

Titel der Masterarbeit / Title of the Master's Thesis

„Deciphering the role of K412 acetylation on HDAC1 function "

verfasst von / submitted by

Selina Knörzer, B.Sc.

angestrebter akademischer Grad / in partial fulfilment of the requirements for the degree of

Master of Science (MSc)

Wien, 2023 / Vienna, 2023

Studienkennzahl lt. Studienblatt / degree programme code as it appears on the student record sheet:	UA 066 877
Studienrichtung lt. Studienblatt / degree programme as it appears on the student record sheet:	Masterstudium Genetik und-Entwicklungsbiologie
Betreut von / Supervisor:	Ao. Univ.-Prof. Dr. Christian Seiser

DANKSAGUNG

Zu Beginn möchte ich mich bei Christian Seiser bedanken, der mir die Möglichkeit gegeben hat, an diesem spannenden Projekt zu arbeiten und Teil einer großartigen Forschungsgruppe zu sein.
Auch bei Valentina Stolz möchte ich mich herzlich bedanken, da sie mein Thema betreut hat und mir jederzeit hilfreich zur Seite stand und immer ein offenes Ohr für Fragen und Diskussionen hatte.
Ein großer Dank gilt auch Terka die immer hilfreiche Tipps hatte und mir mit ihrer Expertise beiseite stand, wenn ich nicht weiter wusste.
Ich möchte mich auch herzlich bei Jelena bedanken, die immer für alle da war und mir ihrer liebevollen und positiven Art den Arbeitsalltag erleichtert hat.
Auch möchte ich mich bei meinen anderen Kollegen Lena, Alex, Gülnihal und Heinz für die schöne gemeinsame Zeit im Labor bedanken.
Auch bedanke ich mich recht herzlich bei Markus Hartl und Wolfgang Reiter von der MPL Mass Spectrometry Facility, die uns bei der Vorbereitung der Proben und der Auswertung der Daten des Interactomes mit ihrem Fachwissen zur Seite standen!
Ein großer Dank geht ebenfalls an Stefan Schüchner, von der MPL Antibody facility, der den monoklonalen HDAC1 K412ac Antikörper hergestellt hat und uns bei der Analyse durchgehend geholfen hat.

Der größte Dank gilt jedoch meinen Eltern, die immer an mich geglaubt haben und mich unterstützt haben. Ohne euch wäre das alles nicht möglich gewesen!

Abstract

Histone deacetylases (HDACs) remove acetyl groups from acetylated lysine residues of histone proteins which results in a more compacted chromatin structure and thereby represses gene expression. Although, HDACs were initially discovered as enzymes that deacetylate histones, they have also been found to deacetylate non-histone proteins. We have recently shown that the class I deacetylase HDAC1 itself is acetylated in the human tumor cell line HAP1. Via mass spectrometry nine lysine residues on HDAC1 have been identified to be target of lysine acetylation. Interestingly, a specific lysine residue, K412, was hyperacetylated upon treatment with the class I HDAC inhibitor MS275 and on catalytically inactive HDAC1. This indicates that HDAC1 itself is a non-histone substrate of HDAC1 and has a potential auto-deacetylation function. These data were recently confirmed in murine T-cells (T. Vcelkova and W. Reiter).

In this study we focused on deciphering the biological function of lysine 412 acetylation on HDAC1. We investigated the influence on its enzymatic activity, protein stability and interacting proteins. Catalytic deacetylase activity of HDAC1 was unaffected by acetylation mimicking (K412Q) and acetylation resistant (K412R) mutations. The mutation of K412 had also no effect on HDAC1 protein stability, which was followed via cycloheximide chase experiment. However, immunoprecipitation experiments suggest that the binding affinity of HDAC1 to its co-repressors SIN3A and HDAC2 is reduced in the acetylation resistant mutant (K412R). HDAC2 co-immunoprecipitation studies again confirmed these results, while we did not see a reduced interaction with the HDAC1 K412R mutant for SIN3A. Investigation of the interactome of HDAC1 via mass spectrometry also showed a trend to reduced interaction of HDAC2 with the K412R mutant in comparison to HDAC1 WT. In addition, proteins involved in DNA damage response showed an increased interaction with HDAC1 K412R. In summary, mutation of lysine 412 affects mostly the interactome of HDAC1 but not the activity or stability of the enzyme.

Finally, we generated a monoclonal mouse antibody that recognizes acetylated K412 on HDAC1 in collaboration with the MPL Monoclonal Antibody facility. The presence and specificity of the antibody was verified on acetyl-lysine immunoprecipitates of HDAC1 CI and HDAC1 CIK412R. The novel HDAC1 K412ac antibody will be instrumental in future analyses of the function of dynamic HDAC1 acetylation.

Zusammenfassung

Histondeacetylasen (HDACs) entfernen Acetyl-Gruppen von acetyliertem Lysin an Histoproteinen und führen dadurch zu einer kompakteren Chromatinstruktur und somit zu einer verringerten Genexpression. Obwohl HDACs zuerst als Enzyme klassifiziert wurden, die Histone deacetylieren, weiß man in der Zwischenzeit, dass sie auch für die Deacetylierung von Nicht-histon-Proteinen verantwortlich sind. Wir haben vor kurzem in der humanen Tumorzelllinie HAP1 gezeigt, dass die Klasse I Deacetylase HDAC1 selbst an spezifischen Lysin Resten acetyliert wird. Mit Hilfe von Massenspektrometrie wurden neun Lysin-Reste des HDAC1-Proteins identifiziert, die Ziel von Acetylierung sind. Interessanterweise lag einer der Lysine Reste, K412, in hyper-acetylierter Form vor, wenn die Zellen mit dem Klasse I HDAC-Inhibitor MS275 behandelt wurden. An katalytisch inaktivem HDAC1 liegt derselbe Lysin-Rest ebenfalls hyper-acetyliert vor. Dies deutet darauf hin, dass HDAC1 selbst ein Nicht-histon-Substrat für HDAC1 ist und somit potenziell eine Autodeacetlyierungsfunktion hat. Diese Daten wurden kürzlich auch in T-Zellen bestätigt (T. Vcelkova und W. Reiter).

In diesem Projekt wollten wir untersuchen, ob die Acetylierung von HDAC1 an K412 eine biologische Funktion hat. Wir haben ihren Einfluss auf die enzymatische Aktivität, die Proteinstabilität und die Interaktion von HDAC1 mit anderen Proteinen untersucht. Die katalytische Aktivität blieb nach Mutation von HDAC1 zu acetylierungs-imitierenden (K412Q) oder acetylierungs-resistenten (K412R) Isoformen unverändert. Desgleichen hatte die Mutation von K412 keinen Einfluss auf die HDAC1-Proteinstabilität. Immunpräzipitationsexperimente deuteten jedoch darauf hin, dass die Bindungsaffinität von HDAC1 zu seinen Partner-Proteinen SIN3A und HDAC2 bei der acetylierungs-resistenten Mutante (K412R) verringert ist. Die Massenspektrometrie-Analyse des HDAC1-Interaktoms zeigte auch eine Tendenz zu einer reduzierten Wechselwirkung von HDAC2 mit der K412R-Mutante im Vergleich zu HDAC1 WT. HDAC2-Koimmunpräzipitationsstudien konnten diese Ergebnisse erneut bestätigen, während für SIN3A keine reduzierte Wechselwirkung mit der K412R Mutante festgestellt werden konnte. Zusammen gefasst verändert Mutation von Lysin 412 hauptsächlich das Interaktom aber nicht die katalytische Aktivität oder Stabilität des HDAC1-Enzyms.

Schließlich haben wir in Zusammenarbeit mit der MPL Monoklonalen Antikörper Facility einen monoklonalen Maus-Antikörper, der acetyliertes Lysine 412 an HDAC1 erkennt, erzeugt. Die Präsenz sowie die Spezifität des Antikörpers wurden mit Hilfe von Acetyl-Lysin-Immunpräzipitaten von HDAC1 CI und HDAC1 CIK412R Zellen nachgewiesen. Der neue HDAC1 K412ac Antikörper wird für zukünftige Analysen der Funktion der dynamischen HDAC1 Acetylierung nützlich sein.

Table of contents

1. Introduction

1.1 Epigenetics

The term epigenetics comprises all kind of gene regulations that are not mediated by the DNA sequence but by a level of control that is independent of the DNA sequence. Epigenetic modifications are mitotically heritable, albeit reversible chromatin modifications that lead to changes in gene expression (Waterland, 2006). They can either be directed by intrinsic or extrinsic (environmental) signals. The epigenetic landscape is responsible for different gene expression patterns from identical DNA in different cell types and organs (Moris et al., 2016). The patterns are stably inherited from mother to daughter cells. Epigenetic gene control results from the formation of distinct chromatin structures (eu/heterochromatin) and DNA methylation (Jaenisch & Bird 2003).

The epigenetic status of a cell determines if certain genes are turned on or off and thereby influence the abundance of distinct proteins in an organism. The epigenetic pattern ensures that each cell produces only the proteins that are required under certain circumstances or during a certain point of development (Moris et al., 2016). Typical examples of epigenetic modifications include the random inactivation of the X-chromosome in females and the imprinting of maternal and paternal gene loci during embryonic development (Chen & Zhang, 2020). The modification of the DNA and its scaffold (histone proteins) as well as several associated proteins define a cells epigenetic landscape and have a major impact on gene expression (Gibney & Nolan, 2010).

1.2 Organization of eukaryotic chromatin and Histone code

In eukaryotes, the DNA is packed in a basic structure called nucleosomes, consisting of histones and DNA. Nucleosomes consist of eight histone proteins (histone octamer), around which the DNA is wrapped twice in pieces of 146 bp (Luger et al., 1997). The positively charged histone proteins interact with the DNA backbone which is negatively charged. The histone octamer is formed by two copies of the core histone proteins H2A, H2B, H3 and H4. H2A and H2B form dimers via coiled coil interactions while H3 and H4 form tetramers via helical interactions (Arents et al., 1991). Histone H1 is not directly associated with the nucleosome, but binds to the linker DNA which is located between two nucleosomes. It helps to coil the nucleosomes together to make a more densely packed DNA (Popova EY & Grigoryev, 2013). This compact structure of DNA wrapped around nucleosomes is dynamic and can be regulated by post-translational modifications (PTMs) and chromatin remodeling complexes. The N-termini of the histone proteins, the so-called histone tails, stick out of the compact nucleosomal

structure, and are in this way accessible for modifications (Bowman & Poirier, 2015). Chromosomes are organized into defined nuclear territories which can be distinguished in euchromatin and heterochromatin. Euchromatin has complex, unique DNA sequences that can be easily transcribed whereas heterochromatin consists mostly of repetitive sequences that are tightly packed and transcriptionally silenced (Tamaru H, 2010; Cremer & Cremer, 2010).

Nucleosome modifications such as acetylation, phosphorylation, methylation or ubiquitination distinguish heterochromatin from euchromatin. The combination of different histone modifications that regulate chromatin structure and therefore transcription is called the histone code. Typical histone marks of euchromatin are acetylated histones H3 and H4 as well as H3K4 methylation. Heterochromatin exists mostly in a hypoacetylated state and exhibits H3K9 methylation and DNA cytosine methylation (Jenuwein & David Allis, 2001). A defining feature of heterochromatin is that it self-perpetuates its transcriptionally repressed state and highly condensed structure on chromosomes in a region-specific manner throughout the cell cycle over generations (Tamaru H, 2010).

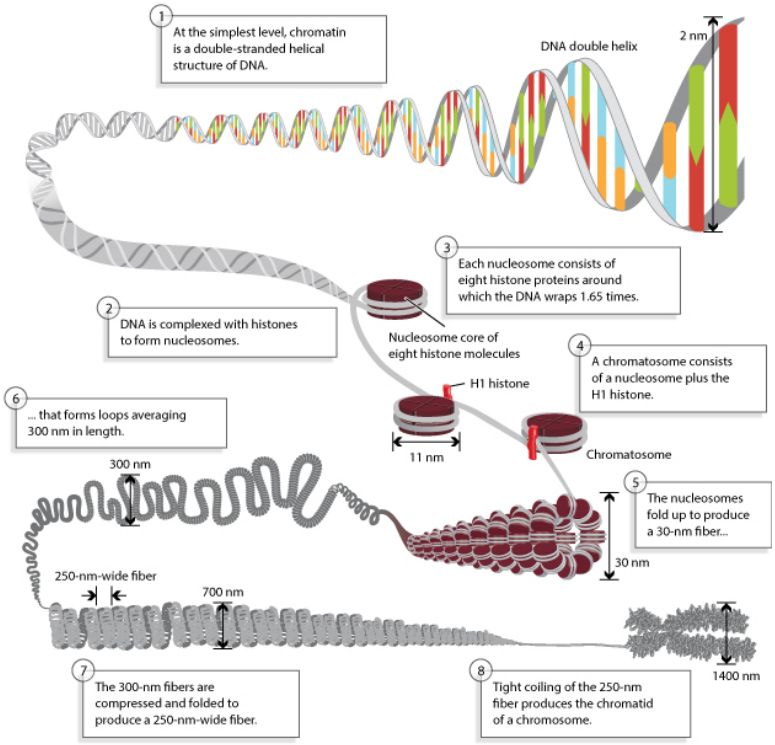

Figure 1. Structural organization of eukaryotic chromatin. The DNA double helix is wrapped around a histone octamer, resulting in the “beads on a string form” of chromatin. Compaction of the nucleosomes results in an approximately 30nm thick chromatin fiber, which can further be packed and condensed into chromosome arms. Figure taken from (Karki, 2020 Cell Biology, Genetics).

1.3 Epigenetic modifications and mechanisms

To establish an epigenetic landscape, distinct enzymes, the so called writers and erasers, are required. Writer enzymes add posttranslational modifications to the histone tails which can be recognized by reader proteins. Basically all chromatin modifications are reversible and can be removed by eraser enzymes (Gillette & Hill, 2015).

1.4 DNA Methylation

If a cytosine base is followed by a guanine base (CpG) in the DNA sequence, the cytosine can be modified by methylation. The methyl group is added at the 5' position of the cytosine by DNA methyltransferases (DNMTs), (Robertson, 2005). Methylation of DNA is a way to silence genes so it contributes to epigenetic silencing of genes (Paszkowski & Whitham, 2001). Usually gene silencing through DNA methylation is (nearly) permanent. An example is the silenced X-chromosomes which not only displays repressive chromatin marks but also methylated DNA. One exception off this phenomenon are CpG islands, which harbor several CpG sequences within a short span of DNA, since these are mostly not methylated. They are found at the 5' ends of housekeeping genes which are permanently active (Caiafa & Zampieri, 2004). DNA methylation also plays a crucial role during development and is a heritable epigenetic mark (Li E & Zhang Y, 2014).

1.4.1 Histone post-translational modifications (PTMs)

The N-terminal tail of histone proteins serves as platform for many different modifications such as acetylation, phosphorylation, methylation, SUMOylation or ubiquitylation. PTMs play a crucial role in regulating the activation and repression of gene transcription (Bowman & Poirier, 2015).

1.4.1.1 Acetylation

Lysine residues with an NH_2 amino group can serve to attach an acetyl group via histone acetyltransferase (HAT) activity (Marzluff & McCarty, 1970). The acetyl group neutralizes the positive charge of the lysines of histones which weakens its electrostatic interaction with the DNA which in turn gets less compacted and more accessible. The incorporation of the acetyl group is reversible and can be removed by histone deacetylase (HDACs), (Verdone et al., 2006). By removing the acetyl mark, HDACs tighten the compaction of the DNA and thereby act as gene repressors. The histone acetylation state is dynamically regulated by HATs and HDACs. Acetylated histones can be recognized by reader enzymes carrying a bromo-domain

(Bannister & Kouzarides, 2011). Hyperacetylated H3 and H4 are indication marks for transcriptionally active gene regions. H3K9ac and H4K16ac can be found at promoters of active genes while enhancers are known to exhibit a high level of H3K27ac (Biterge, 2016).

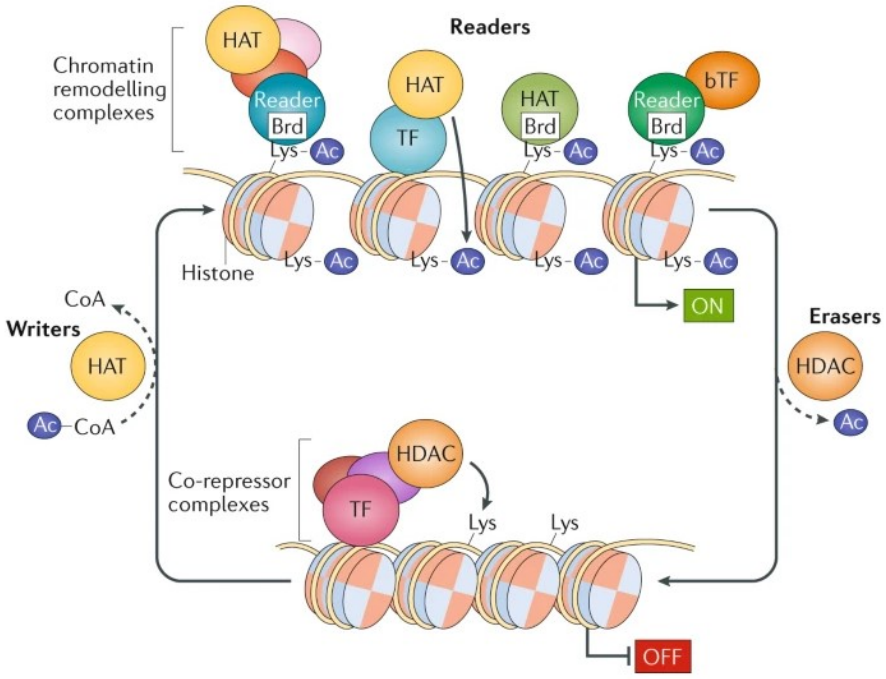

Figure 2. Reversible Histone Acetylation. Lysine residues on histones can be modified by the addition of an acetyl group (acetylation) through the action of enzymes called histone acetyltransferases (HATs). Acetylation of histones leads to a more relaxed, open chromatin structure, making the DNA more accessible to the transcriptional machinery. Conversely, deacetylation of histones, typically by enzymes called histone deacetylases (HDACs), leads to a more tightly packed, closed chromatin structure, which can repress gene transcription. Figure taken from (Ellmeier & Seiser, 2018).

1.4.1.1.1 Acetylation of non-histone proteins

Non-histone acetylation refers to the process by which an acetyl group is added to proteins other than histones. This post translational modification can occur on a wide variety of proteins and has a significant impact on their function and regulation (Choudhary et al., 2014). This process is carried out by the same enzymes (HATs and HDACs) that acetylate and deacetylate histones (Glozak et al., 2005). The balance between acetylation and deacetylation of non-histone proteins is also tightly regulated and plays an important role in a wide range of cellular processes, including transcription, DNA repair, and cell signaling (Narita et al., 2019). Dysregulation of non-histone acetylation has been linked to a number of diseases, including cancer (Singh BN et al., 2010). Acetylation can change the protein's conformation, making it more accessible for other proteins to bind to it, or it can change the protein's localization by altering its interaction with other cellular components. Additionally, it can change the protein's stability by influencing its degradation rate (Kim et al., 2006). Non-histone proteins that are

known to be acetylated include transcription factors, co-activators, chromatin remodelers, and other regulatory proteins that control various cellular processes. One example is transcription factor p53, which is a tumor suppressor protein that plays a critical role in the regulation of cell growth and division. In an acetylated state p53 displays increased stability and DNA-binding ability which results in the activation of p53-dependent transcription (Gu and Roeder, 1997). In cancer cells, the activity of p53 is often decreased due to less acetylation. This allows cancer cells to evade cell cycle arrest and apoptosis, leading to uncontrolled cell growth and proliferation (Reed & Quelle, 2015).

HATs and HDACs are known to be acetylated. This process can modulate their activity, stability, and localization. In the case of HATs, acetylation can enhance their activity by stabilizing the enzyme or by changing its localization in the cell. For example, the HAT p300 is known to undergo autoacetylation on specific lysine residues, which can increase its activity and specificity for certain target proteins (Thompson et al., 2004). On the other hand acetylation of HDACs can inhibit their activity by altering the conformation of the enzyme. For example, HDAC1 and HDAC2 are known to be acetylated on specific lysine residues, which can inhibit their deacetylase activity (Choudhary et al. 2009).

1.4.1.2 Other post-translational modifications

Acetylation occurs exclusively on lysine residues whereas methylation can take place on lysine as well as arginine residues (Bannister & Kouzarides, 2011). The incorporation of a methyl group is carried out by specific histone methyltransferases (HMTs). It does not change the charge of the histone protein but can direct the binding of effector molecules. Therefore histone methylation can be linked to either repression or activation of transcription. For instance, H3K27 di- or trimethylation are known to be repressive chromatin marks while H3K4 di- or trimethylation is predominantly found in active gene regions (Gillette & Hill, 2015).

Serine, threonine and tyrosine residues of histones can serve to attach phosphate groups. The phosphorylation of histones is governed by kinases and phosphatases. Phosphorylation is one of the most common forms of post-translational modifications and regulates many signal transduction pathways (Rossetto et al., 2012). Other forms of post-translational modifications are SUMOylation which refers to the covalent binding of small ubiquitin-like modifiers (SUMO) to lysine residues of histones or other proteins via enzymatic activity akin to the ubiquitylation pathway (Wilkinson & Henley, 2010). In the ubiquitylation pathway the lysine residue of the histone tail gets marked with an ubiquitin group. H2BK123ub1 is known to be involved in transcriptional initiation and elongation while H2AK119ub1 is linked to gene silencing (Bannister & Kouzarides, 2011).

1.5 Histone deacetylases

HDACs can be divided into 4 classes (I, II, III and IV) based to their homology with yeast enzymes (Li, Zhu 2014). Class I HDACs (HDAC1, 2, 3 and 8) are localized in the nucleus. They are found as homo- or heterodimers and have a wide substrate specificity (Moser et al., 2014). Class II HDACs (HDAC4, 5, 6, 7, 9, and 10) are localized in the cytoplasm and the nucleus. They are found as homo- or heterodimers, with a more restricted substrate specificity than class I HDACs (Thiagalingam et al., 2006). Class III HDACs (Sirtuins 1-7) are NAD+ dependent enzymes which can be found in the nucleus and the cytoplasm and exhibit a restricted substrate specificity (Vaquero et al., 2007). HDAC11 is the only member of class IV HDACs and is structurally different from the other classes (Voelter-Mahlknecht et al., 2005).

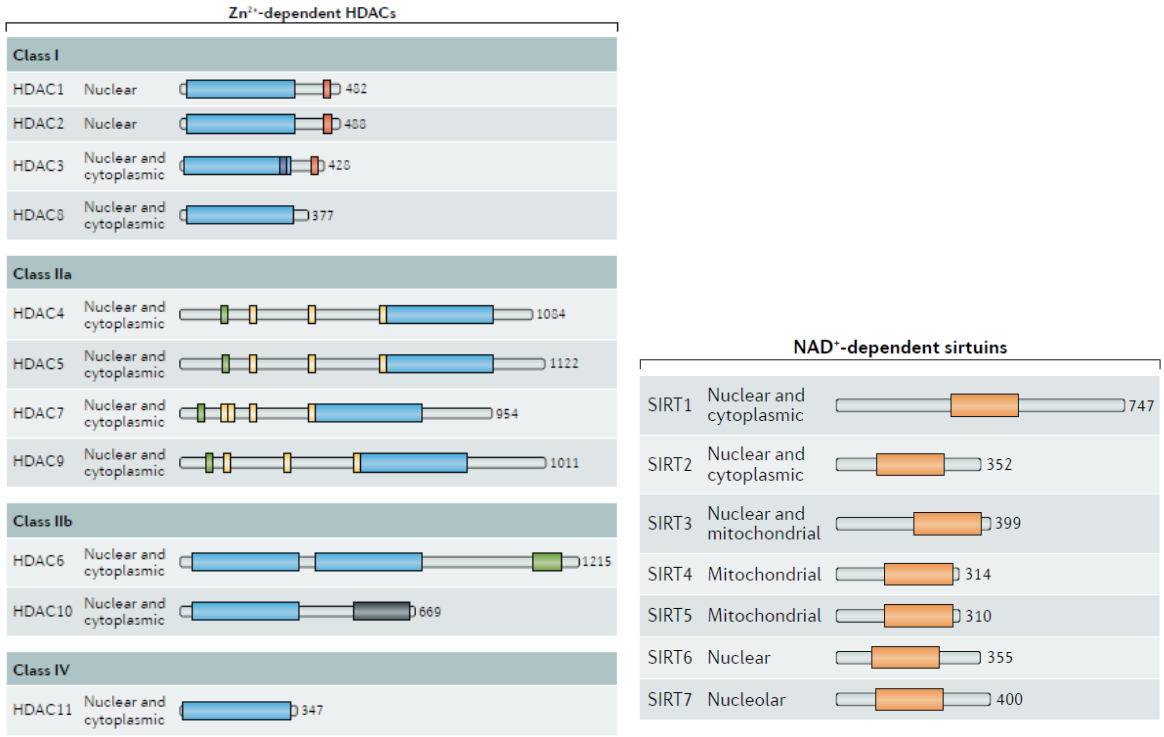

Figure 3. Structural classification of human HDACs and their localization. HDACs are classified into four classes: class I, class II, class III, and class IV. Class I, II and IV HDACs are Zn2+-containing enzymes that use acetyl- CoA as a co- substrate while the class III sirtuins use an NAD+-dependent mechanism. For each HDAC protein the total number of amino acids is indicated. Additionally, the intracellular localization of the distinct HDACs is shown. Figure taken from (Ellmeier & Seiser, 2018).

1.5.1 HDAC1 and HDAC2

HDAC1 and HDAC2 are the products of a gene duplication (Khier et al., 1999). The catalytic domains of HDAC1 and HDAC2 are structurally similar and share a high degree of sequence homology. They are located in the N-terminus of the protein and contain a zinc-binding site, which is composed of two histidine residues and one cysteine residue. These residues

coordinate the zinc ion, which is essential for the enzymatic activity of the enzyme. An HDAC association domain (HAD) partly overlaps with the catalytic domain which is important for homo- or heterodimerization of HDAC1 and HDAC2 (Moser et al., 2014; Brunmeir et al. 2009). It has been shown that, in some cases, a decreased expression of either HDAC1 or HDAC2 can be compensated by upregulation of the other paralog (Winter et al., 2013). To exert their deacetylase activity, HDAC1 and HDAC2 require the interaction with co-repressor complexes. Sin3A, CoREST and NuRD belong to the best-characterized complexes that function together with HDAC1/2 (Millard et al., 2013).

HDAC1 and HDAC2 are known to be involved in the regulation of chromatin structure through the deacetylation of histones, which results in the compaction of chromatin structure and repression of gene expression. However, they were also shown to co-localize with HATs on active genes and the binding of both is positively associated with transcription and RNA-polymerase II levels (Wang et al. 2009). Furthermore, they play a role in the regulation of cell cycle progression, cell differentiation and cell survival. HDAC1 and HDAC2 are highly expressed in cancer cells and are thought to play a role in the development and progression of cancer (Kim HJ et al., 2011). They can be regulated by different mechanisms, such as phosphorylation, sumoylation, ubiquitination and acetylation (Moser et al., 2014). HDAC1 and HDAC2 are known to undergo acetylation on specific lysine residues, which can inhibit their deacetylase activity. This regulation allows for fine-tuning of their activity in response to different stimuli and conditions. Six lysine residues within the HDAC1 enzyme have been shown to be targets of acetylation, which has a negative impact on its enzymatic activity (Qiu et al. 2006).

1.6 Association of HDAC1/2 with co-repressor complexes

HDAC1 and HDAC2 are known to interact with numerous proteins, including transcription factors, co-activators, chromatin remodeling proteins, and other regulatory proteins. These interactions play a critical role in the regulation of gene expression. In order to perform their full deacetylase activity HDAC1 and HDAC2 work as part of multiprotein co-repressor complexes. They are known to be part of the SIN3 (switch-independent 3), CoREST (co-repressor of REST) and NuRD (nucleosome remodeling and deacetylase) complexes (Millard et al., 2013). Corepressor complexes are composed of multiple proteins which are recruited to the promoter region of genes by transcription factors. HDAC1/2 is the catalytic core of the complex while the co-repressor proteins guide HDAC1/2 to the chromatin (Zhang et al., 1999). The Sin3-histone deacetylase complex is composed of several proteins, including either Sin3A or Sin3B. Both proteins contain a HID domain to interact with HDAC1/2 (Laherty et al., 1997). The CoREST complex also consists of multiple proteins including CoREST, MeCP2, SIN3,

HDAC1 and HDAC2 (Brunmeir et al., 2009). It interacts with other proteins such the chromatin remodeling complex SWI/SNF, which is involved in the regulation of gene expression by remodeling the chromatin structure (Battaglioli et al., 2002). In addition to its role in gene regulation, the CoREST complex has also been found to play a role in the regulation of neuronal development and neural plasticity, by interacting with several proteins such as REST (RE1-Silencing Transcription factor) and MeCP2 (Methyl CpG binding protein 2), (Brunmeir et al. 2009). The histone demethylase LSD1 (Lysine Specific Demethylase 1) has been identified as a component of the CoREST complex. This complex functions to repress gene expression by both deacetylating histones and removing methyl groups from lysine residues (Yang et al., 2006). The NURD complex includes the proteins Mi-2/CHD3 and Mi-2/CHD4 which function as ATP-dependent chromatin remodelers (Clapier & Cairns, 2009). They recruit HDACs and other corepressor proteins to the promoter region of genes. The metastasis associated proteins MTA1, MTA2 or MTA3, mediate the interaction with HDACs or with DNA as well as transcription factors and coregulators. The NURD complex is known to be involved in cell growth, cell differentiation, and cell survival. Like CoREST, the NURD complex plays a role in the regulation of neuronal development and neural plasticity (Moon et al., 2017).

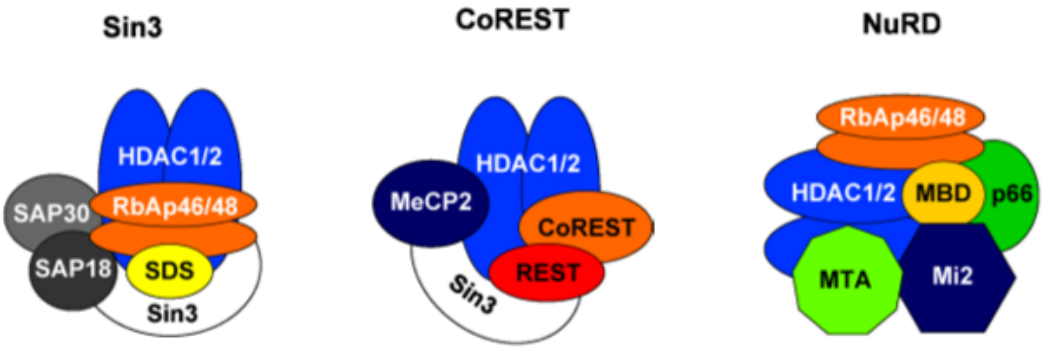

Figure 4. HDAC1/2 and its association with corepressor complexes. HDAC1 and HDAC2 are associated with various corepressor complexes which help to repress gene expression by remodeling chromatin structure. SIN3, CoREST and NURD are among the best-characterized corepressor complexes that are associated with HDAC1/2. The SIN3 complex consists of HDAC1, HDAC2, SIN3, RbAp46, RbAp48, SAP18, SAP30 and SDS3. RbAp46, RbAp48, HDAC1 and HDAC2 are also found in the NuRD complex, in addition with the NuRD specific factors MTA, Mi-2, p66 and MBD. The CoREST complex is comprised of CoREST, MeCP2, SIN3, HDAC1 and HDAC2. HDAC1/2 carry out the enzymatic activity while the other components guide the complex to the DNA. Figure taken from (Brunmeir et al., 2009).

1.7 HDAC inhibitors

Histone deacetylase inhibitors (HDACi) are a class of compounds that are able to inhibit the activity of histone deacetylases (HDACs). They disrupt the normal activity of HDACs, leading to the accumulation of acetylated histones and other proteins, which leads to changes in chromatin structure and gene expression. HDACi have been found to have a wide range of effects on cellular processes, including cell growth, cell differentiation, cell survival, and cellular signaling (Miller et al., 2003). They have been investigated for their potential as therapeutic agents for a variety of diseases, including cancer, neurodegenerative disorders, and inflammatory diseases (Egger et al., 2004). There are several classes of HDAC inhibitors that have been identified, including hydroxamic acids, cyclic peptides, and benzamides, which have different mechanisms of action (Miller at el., 2003). Examples are: Vorinostat a hydroxamic acid-based HDAC inhibitor that has been FDA-approved for the treatment of cutaneous T-cell lymphoma (CTCL); Romidepsin a cyclic peptide-based HDAC inhibitor that has been FDA-approved for the treatment of CTCL; Panobinostat a benzamide-based HDAC inhibitor that has been FDA-approved for the treatment of multiple myeloma in combination with other drugs (Botrugno et al., 2012).

HDACi are being studied in combination with other cancer treatments like chemotherapy, radiation, and immunotherapy (Suraweera et al., 2018). Since HDACs are known to be overexpressed in different types of cancers, HDACi have shown promise as a potential cancer therapy. However, a broad-spectrum of HDAC inhibitors are associated with severe side effects for patients due to their broad mode of action (Botrugno et al., 2012). The pan-HDACi that are currently in use show almost no specificity to any of the eleven zinc-dependent HDACs which may be the cause for the undesired side effects. Thus, use of more specific HDACi could be beneficial. Taken together, more research is needed to fully understand their mechanisms of action, and to identify the most appropriate uses of HDACi in the clinical setting (Egger et al., 2004).

1.8 Aim of the study and experimental design

The main goal of this study was to decipher the role of lysine acetylation on HDAC1 function. Via mass spectrometry analysis our lab has recently revealed that HDAC1 itself is a novel non-histone target for acetylation in the human tumor cell line HAP1 (Hess, Moos et al, 2022). Strikingly K412 was hyperacetylated upon treatment with the class I HDAC inhibitor MS275 and at the catalytically inactive mutant HDAC1 H141A, suggesting auto-deacetylation of HDAC1 as a potential mechanism. These data were confirmed in murine T-cells (Vcelkova and Reiter). To study the impact of HDAC1 acetylation on K412, our lab created HAP1 cell lines expressing FLAG-tagged HDAC1 isoforms with lysine mutations preventing (HDAC1 K412R) or mimicking (HDAC1 K412Q) acetylation of lysine residue K412 instead of the endogenous wildtype protein (Cvetcovic and Vcelkova). With these cell lines and three control cell lines expressing FLAG-tagged HDAC1 wildtype protein (HDAC1 WT), catalytically inactive HDAC1 (HDAC1 CI) and catalytically inactive HDAC1 with K412 acetylation preventing mutation (HDAC1 CI K412R) I performed a detailed biochemical analysis. Using FLAG co-immunoprecipitation experiments I investigated whether the 412R and 412Q mutants are still incorporated into the multi subunit corepressor complexes SIN3A, NURD and COREST. Besides, the activity of the acetyl HDAC1 mutants was measured using 3H-acetate-labelled chicken erythrocyte histones as substrates. Furthermore, I followed the stability of HDAC1 412R, 412Q, CI and WT proteins by cycloheximide time course experiments.

Another goal of my project was to characterize an antibody specifically directed against acetylated lysine K412. To identify and analyze HDAC1 proteins acetylated at K412 we set out to generate a monoclonal HDAC1 K412ac antibody in collaboration with Stefan Schüchner (MPL antibody facility). Therefore mice have been immunized with the peptide encompassing amino acids 408/409 to 415/416 with acetylated K412, which was either linked via the C-terminus or the N-terminus with keyhole limpet hemocyanin (KLH). Mice that produced antibodies against the injected peptide have been identified by ELISA. After a booster immunization, selected positive mice have been sacrificed to produce monoclonal antibodies via cell fusion and single cell dilution. In parallel, I enriched isolated acetylated proteins by performing acetyl-lysine immunoprecipitation experiments. The precipitates have then been used to verify the presence and specificity of antibodies in the mouse sera, polyclonal and monoclonal supernatants.

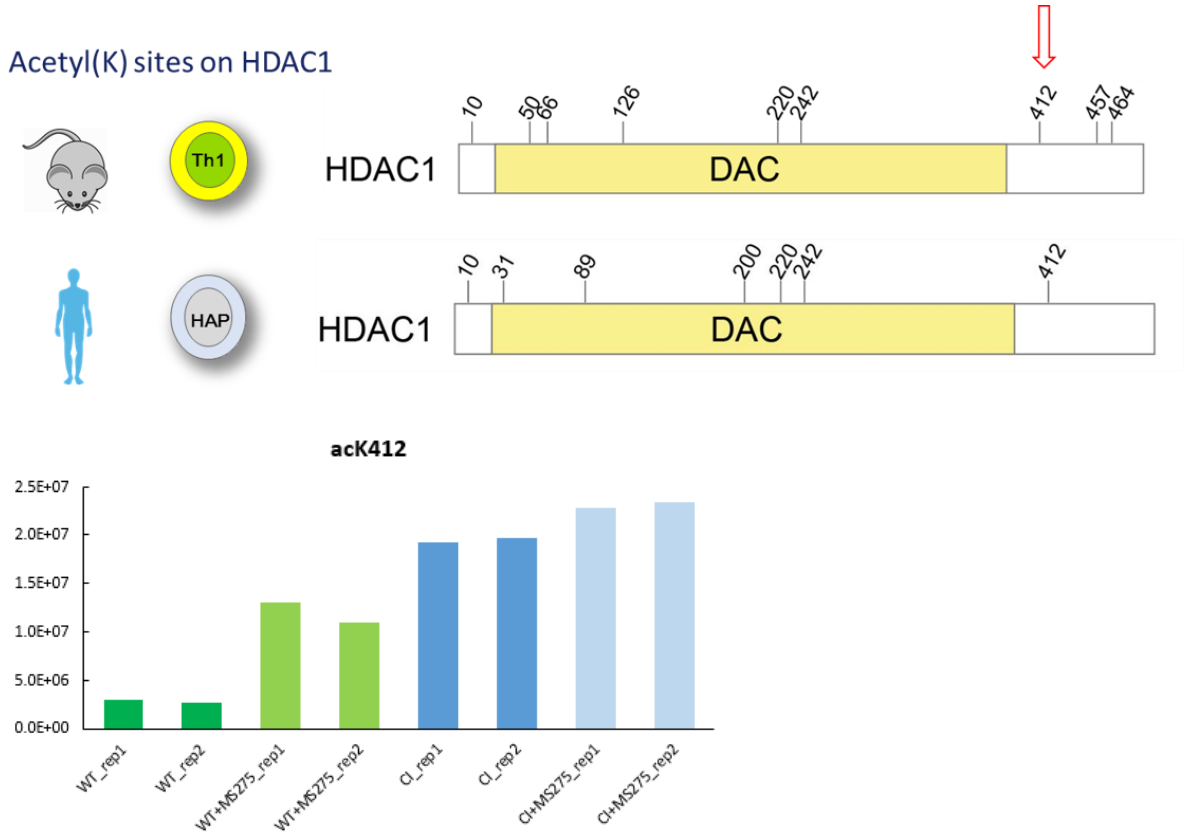

Figure 5. Acetylated lysine sites on HDAC1. Acetylated lysine sites on HDAC1 have been identified via mass spectrometry including K10, K50, K66, K126, K220, K242, K412, K457, K464 in Th1 cells from mice and K10, K31, K89, K200, K220, K242 and K412 in HAP cells. Lower panel: Regulation of K412 acetylation by MS-275 and HDAC1 inactivation examined by mass spectrometry.

Figure 5 shows that lysine 412 site was more acetylated in WT cells treated with the HDAC inhibitor MS275 (which inhibits HDAC1, HDAC2 and HDAC3) compared to untreated WT cells. In the catalytically inactive mutant (CI), even without MS275 treatment, lysine 412 was more acetylated than WT cells treated with MS275. Interestingly, treatment of the CI mutant with MS275 does not lead to a further increase of K412 acetylation compared to untreated CI cells. This data indicates that HDAC1 is a potential non-histone target of HDAC1. (Terka Vcelkova, Wolfgang Reiter and Natalija Siomonovic, unpublished data).

2. Material and methods

2.1 Work with mammalian cells

All steps were conducted under sterile conditions in a laminar flow hood.

2.1.1 Cell lines

Table 1. Cell lines used for experiments.

Cell line	Organism	Tissue	Cell type	Genotypes / Features
HAP 1 WT	Homo sapiens	Male CML: KBM-7	fibroblast-like	near haploid
HAP1 HDAC1 WT	Homo sapiens	Male CML: KBM-7	fibroblast-like	WT HDAC1-FLAG transgene in the AAVS1 locus
HAP1 HDAC1 K412R	Homo sapiens	Male CML: KBM-7	fibroblast-like	HDAC1 K412R-FLAG transgene in the AAVS1 locus; lysine 412 mutated to arginine
HAP1 HDAC1 K412Q	Homo sapiens	Male CML: KBM-7	fibroblast-like	HDAC1 K412Q-FLAG transgene in the AAVS1 locus; lysine 412 mutated to glutamine
HAP1 HDAC1 CI	Homo sapiens	Male CML: KBM-7	fibroblast-like	HDAC1 H141A-FLAG transgene in the AAVS1 locus; histidine 141 mutated to alanine
HAP1 HDAC1 CI 412R	Homo sapiens	Male CML: KBM-7	fibroblast-like	HDAC1 H141A-K412Q-FLAG transgene in the AAVS1 locus; histidine 141 mutated to alanine and lysine 412 mutated to glutamine

2.1.2 Thawing of frozen cells

Frozen cell vials were transferred into an icebox and then quickly thawed in a 37°C water bath. Afterwards the thawed cells were transferred into a 15 ml-falcon tube and resuspended with 5ml IMDM medium. The resuspended cells were centrifuged at 1200rpm for 5 minutes at room temperature, the supernatant was carefully aspirated, to remove the toxic DMSO. The cell

pellet was resuspended in 1 ml fresh media. Finally, the cells were seeded dropwise in a dish of the appropriate size in the desired dilution. The plated cells were kept in IMDM medium at 37°C, 5% CO_2.

2.1.3 Cell splitting

The cells were kept in culture until they were 80-90% confluent. After reaching the confluency, the cells were split in a ration between 1:3 and 1:10. First, the medium was aspirated from the dish and the plate was washed twice with 1 ml sterile PBS to remove dead cells. Next, the cells were detached from the plate using 1ml trypsin for 10cm plates and 1.5ml trypsin for 15cm plates. After incubating for 3 minutes at 37°C the cells were checked under the microscope to confirm successful detachment. To stop the trypsination reaction the cells were resuspended with at least the triple amount of media. At last, the cells were transferred into a 15 ml-falcon tube and spun down for 5 min at 1200 rpm. The cell pellet was resuspended in an appropriate amount of IMDM media and added on the fresh plate dropwise.

2.1.4 Cell freezing

The media was removed from the plate and the cells were washed with 1ml PBS. Subsequently, the cells were trypsinated with 1ml trypsin for 3 minutes in the incubator. To transfer the cells into a 15ml falcon tube 4ml IMDM media were added. The cells were spun down for 3-5 min at 300 rcf and the supernatant was removed. Finally, 1800 µl of FBS and 200 µl 10% DMSO were added. Then the cells were distributed in cryovials (1ml per tube) and frozen at -80°. Afterwards they were stored in liquid nitrogen.

2.1.5 Cell harvesting

Before harvesting the cells were grown on a 15cm plate. First, the media was removed from the plate and washed twice with 5ml cold PBS. The cells were harvested in 5ml PBS with a cell scraper and collected in a Falcon tube. Subsequently, the cells were centrifuged for 5 min at 1200 rpm at 4ºC. The supernatant was discarded and the pellet was resuspended in 1ml PBS and transferred into 1ml microcentrifuge tubes. Again the cells were centrifuged at 4°C, 0.3 rcf for 5 minutes. At last, the supernatant was aspirated, and the cell pellets were stored at -20ºC.

2.1.6 Cycloheximide treatment

The cells were grown on a 10 cm dish. When confluent they were trypsinated and resuspended in an appropriate volume of IMDM media. To count the cells, 10µl of the cell suspension was mixed with 10µl of trypan blue stock solution and transferred in a hemocytometer. The amount of living cells was determined with a cell counter. The desired amount (250.000cells/well) was plated on a 48 well plate in 1ml of IMDM media and incubated overnight. On the next day, the cells were treated with 300µg/ml of Cycloheximide dissolved in DMSO. The negative control was treated with DMSO only. The cells were harvested after 0, 2, 4, 6, and 8 hours as described in the "harvesting" section. Subsequently, 100µl of PBS plus 0.1µl of eBioscience fixable viability dye eFluor 506 (1:1000 dilution) was added per sample. The samples were incubate for 10 min at 4°C in the dark. Then, 1ml PBS was added to the sample which was then centrifuged at 450 rcf at 4°C for 4 minutes. The supernatant was removed and cells were fixed using the eBioscience Foxp3 Transcription Factor Staining Buffer Set according to manufacturer's protocol. After fixation, samples were incubated with anti-FLAG M2 antibody for 1 hour at 4°C in the dark (1:500 dilution) (Sigma-Aldrich) and subsequently stained using an APC-conjugated goat anti-mouse IgG antibody (1:200 dilution) (Biolegend) for 1 hour at 4°C in the dark. Then again, 1ml PBS was added and the sample was centrifuged at 450 rcf at 4°C for 4 minutes. The supernatant was removed and the samples were washed with 1ml PBS one more time. Cells were resuspended in 200µl PBS and analyzed by Flow cytometry using a Beckman Coulter CytoFLEX S2.

<u>IMDM medium</u>

500 ml Iscove's Modified Dulbecco's Medium (IMDM) (Gibco, Thermo Fisher Scientific)

10% Fetal Bovine Serum (FBS)

1% L-Glutamine

1% Penicillin/Streptomycin

<u>Trypsin/ EDTA (Sigma-Aldrich)</u>

0.1% trypsin

2% EDTA

10x PBS

8% sodium chloride

0.2% potassium chloride

0.2% monopotassium phosphate

1.11% disodium hydrogen phosphate

Diluted in dH2O and pH adjusted to 7.4 with NaOH

2.2 Work with proteins

2.2.1 Protein extraction of cells with freeze and thaw method

Cell pellets were thawed on ice and dissolved in an appropriate amount of Hunt buffer supplemented with inhibitors (see in the list below). This was followed by three freeze and thaw cycles: frozen in liquid nitrogen and thawed at room temperature, frozen in liquid nitrogen and thawed at 37°C, frozen in liquid nitrogen and thawed during centrifugation for 30 minutes at 4°C with 14,000rpm. The supernatant was transferred to a new 1.5ml microcentrifuge tube and the protein concentration was measured via Bradford protein assay.

Hunt Buffer

20 mM Tris-HCl, pH 8.0

100 mM Sodium chloride

1 mM EDTA

0.5% NP-40

Protease and phosphatase inhibitors recipe

1x Complete protease inhibitor cocktail (Roche)

100 µM PMSF

10 mM Sodium fluoride

10 mM β-glycerophosphate

100 µM Sodium molybdate

100 µM Orthovanadate (before use, activated at 95°C for 5 minutes)

2.2.2 Bradford protein assay

The protein concentration was determined via Bradford protein assay. Therefore, the Bradford stock solution (Bio-Rad) was diluted 1:5 in dH2O. In the following step, 1ml of Bradford solution was mixed with 1µl of the sample. For blank 1ml Bradford solution was mixed with 1µl Hunt buffer + inhibitors. All samples were measured in duplicates and the average concentration was calculated. The absorbance at 595nm was determined with a photometer. The calculation

of the protein concentration was executed as followed: absorbance*10 = µg/µl. Only samples measured in a range between 0.1 - 0.5 were used, in case of a higher or lower concentration the measurement was repeated.

2.2.3 Extraction of nuclear proteins via high salt method

The buffers were prepared as described below and supplemented with inhibitors (2.2.1). Cells were grown on a 15cm plate. First, the media was removed from the cell culture dishes and the cells were scrapped off the plate in 5ml ice cold PBS. The cell suspension was centrifuged at 1500 rpm for 5 minutes at 4°C. The pellet was resuspended in 1 ml of cold PBS and transferred into a 1.5ml microcentrifuge tube. Another centrifugation step followed at 2500 rpm for 5 minutes at 4°C. The supernatant was aspired and the pellet was dissolved in an appropriate amount of sucrose buffer (adjusted to cell pellet size). In a further centrifugation step the nuclei were pelleted at 2500 rpm for 5 minutes at 4°C. The supernatant, containing the cytosolic fraction, was kept for further analysis. Next, the nuclear pellet was washed twice with 1 ml of sucrose buffer without NP-40 and centrifuged at 2500 rpm for 5 minutes at 4°C. Following, the wash buffer was removed and the nuclear pellet was carefully resuspended in in low salt buffer (size of pellet was estimated and the same amount of buffer was added) by finger vortexing. Further, an equal amount of high salt buffer was added by slowly mixing the suspension with the pipette tip. The samples were incubated for 2-3 hours shaking with 1000 rpm at 4°C. At last, the samples were centrifuged at 14000rpm for 15 minutes at 4 °C. The supernatant, containing the nuclear extract, was transferred into a new microcentrifuge tube. The protein concentration was measured via Bradford protein assay (2.2.2).

<u>Sucrose buffer (prepared twice, either with NP-40 or without NP-40)</u>

0.32M sucrose

10mM Tris-HCl, pH 8.0

3mM calcium chloride

2mM magnesium acetate

0.1mM EDTA

(0.5% NP-40)

Low salt buffer

20mM Hepes, pH 7.9

1.5mM magnesium chloride

20mM potassium chloride

0.2mM EDTA

25% glycerol (v/v)

High salt buffer

20mM Hepes, pH 7.9

1.5mM magnesium chloride

800mM potassium chloride

0.2mM EDTA

25% glycerol (v/v)

1% NP-40

2.2.4 SDS-PAGE gel electrophoresis

Proteins were separated according to their size by SDS-PAGE gel electrophoresis. Therefore, a discontinuous SDS-polyacrylamide gel was prepared. To do so the glass plates were assembled, at first the separation gel was filled between the spaces and covered with isopropanol. After polymerization of the separation gel, the stacking gel was prepared and a comb was inserted. After polymerization of the stacking gel the comb was removed such that the samples could be loaded. Gels were cast in Bio-Rad Mini Protean apparatus which was filled with 1 × SDS running buffer. For sample preparation, 20µg of protein extract were filled up to 15µl Hunt buffer + inhibitors (2.2.1) and 5µl SDS with DTT was added. Before loading, the samples were incubated at 95°C for 5 minutes. Next to the samples, 7µl Precision Plus Protein Dual Color (Bio-Rad) was loaded. The proteins were separated on the polyacrylamide gels at constant current (20mA) until they reached the separation gel, then the current was increased up to 30-35mA.

10% SDS separation gel (4 gels)

5.3 ml 30% Acrylamide (Bio-Rad)

4 ml 4x Running gel buffer

6.7 ml H_2O

6.4 µl TEMED

80 µl 20% APS

5% stacking gel (4 gels)

1.3 ml 30% Acrylamide (Bio-Rad)

4 ml 2x Stacking gel buffer

3 ml H_2O

8 µl TEMED

40 µl 20% APS

4x Running gel buffer (500 ml)

90.89 g TRIS (base)

350 ml dH_2O

Adjust pH to 8.8 with acetic acid

20 ml SDS (10% stock)

Ad to 500 ml with dH_2O

2x Stacking gel buffer (500 ml)

15.44 g TRIS (base)

350 ml dH_2O

Adjust pH to 6.8 with acetic acid

10 ml SDS (10% stock)

Ad to 500 ml with dH_2O

Ammonium persulfate (APS)

20% APS diluted in dH_2O

Sodium-dodecyl sulfate (SDS)

20% SDS diluted in dH_2O

SDS loading dye

100 mM Tris/HCl pH 6.8

20% Glycerol

0.01% Bromophenol blue

10% β-mercaptoethanol

5% SDS

Diluted in dH_2O

10x Running Buffer

14.4% Glycine

3% Tris/HCl

1% SDS

Diluted in dH_2O

2.2.5 Western blotting (wet transfer)

After separating the proteins on the discontinuous SDS-polyacrylamide gel they were transferred onto a nitrocellulose membrane using the wet transfer method. The wet blot assembly was carried out as described in the list below. The wet blot sandwich was soaked in wet transfer buffer and added into a blotting cassette (Bio-Rad). The blotting cassette was placed into a tank-blotter (Bio-Rad) filled with the same buffer. The blotting was performed at

250mA for 2 h at 4°C. After the wet blot transfer, the membrane was incubated with 1x Ponceau staining solution for 5 minutes at room temperature. Subsequently, the membrane was washed with ddH2O to remove the excess dye. To prevent unspecific binding, the membrane was incubated in blocking solution for at least 30 minutes at room temperature, shaking.

For Western blotting the following materials were assembled in the given order:

Sponge

3MM Whatman paper

Nitrocellulose membrane (Amersham Protran, GE Healthcare)

SDS-PAGE gel

3MM Whatman paper

Sponge

Wet transfer buffer

25mM Tris-HCl

190mM glycine

20% methanol

10x Ponceau S

2% Ponceau S

30% trichloracetic acid

30% sulfosalicylic acid

Blocking solution

1% Milk powder

1% Polyvinylpyrrolidone

0.1% Tween-20

0.02% Sodium azide

10% 10x PBS

Diluted in dH2O

2.2.6 Immunodetection of Western blots

After blocking, the membrane was transferred into a 50ml Falcon tube with the primary antibody which was diluted in 5ml blocking solution (dilution is depicted in the table below, 2.2.7). The primary antibody was incubated overnight at 4°C under constant rotation. On the next day, the membrane was washed three times for 5 minutes with PBS-T. In the next step, the secondary antibody was incubated (diluted 1:10 000 in PBS-T) for 1h at room temperature shaking. Afterwards, the membrane was washed again three times for 5 minutes with PBS-T. For developing, the ECL Western blotting detection reagents (GE Healthcare) were used: 1ml Detection Reagent 1 was mixed with 1ml Detection Reagent 2 and pipetted onto the membrane. The blot was developed on the Fusion FX7 Spectra machine (Vilber). Quantification of specific bands was carried out with ImageJ.

2.2.7 List of antibodies

Table 2. Primary antibodies used in the study.

Primary antibody	Species	Company	Dilution
FLAG M2 F1804	mouse	Sigma Aldrich	1:1.000
HDAC1 Sat208	rabbit	Seiser Lab	1:10.000
HDAC1 10E2	mouse	Seiser Lab	1:1.000
HDAC2 3F3	mouse	Seiser Lab	1:1.000
MTA2 276	mouse	Sigma Aldrich	1:1.000
Sin3A sc-767 (for IP)	rabbit	Santa Cruz	1:1.000
Sin3A ab3479 (Western blot)	rabbit	Abcam	1:1.000
β-Actin A5316	mouse	Sigma Aldrich	1:1.000
CoREST 07-455	rabbit	Millipore	1:1.000
Vinculin	rabbit	Abcam	1:1.000

Table 3. Secondary antibodies used in the study

Secondary antibody	Species	Company	Dilution
Anti-mouse	goat	Jackson Laboratories (124594)	1:10.000
Anti-rabbit	goat	Jackson Laboratories (129411)	1:10.000

2.2.8 FLAG immunoprecipitation

For FLAG immunoprecipitation, 40µl of Anti-FLAG M2 magnetic beads (Sigma Aldrich) were used per sample. The beads were washed three times using 500µl TBS + inhibitors per wash step. Between the wash steps the tubes was inverted several times, spun down and the supernatant was aspirated using a magnetic rack (Invitrogen). After the final wash step all supernatant was removed. In the next step, the beads were blocked with 100µl blocking solution (Hunt buffer +Inhibitor with 10% BSA (10mg/ml)) per sample for 30min at 4°C on a rotor (20rpm). Per pulldown, 300-500µg of whole protein extract were used in a total volume of 300µl, the samples were filled up with Hunt buffer + inhibitors. After 30 minutes of beads blocking the tubes were placed on the magnetic rack such that the blocking solution could be removed. Subsequently, the protein extract was added and the samples were incubated overnight at 4°C with 20rpm. On the next day, the samples were centrifuged with a mini benchtop centrifuge and placed on the magnetic rack to aspire the supernatant. This was followed by three washing steps with TBS: 2x 5 minutes, 4°C with 20-25rpm, 1x 15 minutes, 4°C with 20-25rpm. In the last step the supernatant was fully aspirated. To elute the FLAG-tagged protein, 30µl of SDS-PAGE sample buffer (no DTT) was added and incubated 5 minutes at 60°C. The eluate was transferred into a new tube and 10µl of SDS loading dye with DTT was added. The sample was either stored at -20°C until use or directly used for Western blot analysis.

TBS

200mM Tris Base

1500mM NaCl

Diluted in dH_2O

Adjust pH to 7.6 with 12 N HCl

2.2.9 HDAC2 Co-immunoprecipitation

HDAC2 co-immunoprecipitation was performed using monoclonal HDAC2 3F3 antibody (Seiser Lab) and protein G-beads (anti-mouse). In the first step, 500µg of whole protein extract were incubated with 4µg of antibody in 300µl total volume for 1h rotating at 4°C. For each sample, 30µl of G-beads were used. The beads were washed three times with Hunt buffer and afterwards incubated for 1h in blocking solution (Hunt buffer +Inhibitor with 10% BSA (10mg/ml)) at 4°C rotating. After blocking, the supernatant was removed and the protein extract was added to the beads. The samples were incubated overnight at 4°C rotating (20rpm). On

the next day, the supernatant was removed and three wash steps followed: 2x 5 minutes with TBS at 4°C with 20-25rpm, 1x 15 minutes with TBS at 4°C with 20-25rpm. Protein was eluted from the beads as described in FLAG immunoprecipitation (2.2.8).

2.2.10 SIN3A Co-immunoprecipitation

SIN3A co-immunoprecipitation was performed using SIN3A antibody (Santa Cruz) and protein A-beads (anti-rabbit). In the first step, 500µg of whole protein extract were incubated in 4µg of antibody in 300µl total volume for 1h rotating at 4°C. For each sample, 30µl of A-beads were used. The beads were washed three times with Hunt buffer and afterwards incubated for 1h in blocking solution (Hunt buffer +Inhibitor with 10% BSA (10mg/ml)) at 4°C rotating. After blocking, the supernatant was removed and the protein extract was added to the beads. The samples were incubated overnight at 4°C rotating (20rpm). On the next day, the supernatant was removed and three wash steps followed: 2x 5 minutes with TBS at 4°C with 20-25rpm, 1x 15 minutes with TBS at 4°C with 20-25rpm. Protein was eluted from the beads as described in FLAG immunoprecipitation (2.2.8).

2.2.11 Immunoprecipitation of Acetylated Protein with Anti-acetyl Lysine Agarose

27µl of the anti-acetyl lysine agarose (Immunechem ICP0388-5M6) was washed in a 1.5 mL vial with 1mL PBST three times, using the micro-centrifuge at a speed around 1000 rpm for 2 minutes. The supernatant was aspirated. In this step the glycerol was removed. In the next step the anti-acetyl lysine agarose was washed twice with 1mL of 0.1M NaH_2PO_4 + 1M NaCl and then again with 1mL PBST. Next, the cell lysate was added (1mg of protein was used) to the anti-acetyl lysine agarose beads and the samples were incubated on a rotor shaker at 4°C overnight. After incubation, the agarose beads were washed with PBST four times, through repeating centrifugation and aspiration. For Western blot analysis 30µl of SDS without DTT were added to the beads. Afterwards, the samples were vortexed and boiled for 2 minutes. Then, the beads were centrifuged at 5000rpm for 2 minutes and the supernatant was used for analysis by following the normal Western blot procedure (2.2.5).

2.2.12 HDAC activity assay with ^{3}H-acetate labeled histones

To measure histone deacetylase activity of acetyl HDAC1 mutants ^{3}H acetate-labeled chicken erythrocyte histones (provided by Gerald Brosch, University of Innsbruck) were used. For the experiment, immunoprecipitated FLAG-tagged HDAC1 proteins were utilized. On day two of

the FLAG immunoprecipitation experiment (2.2.8) the beads were resuspended in 300µl of Hunt buffer + inhibitors after the washing steps. From the suspension, 2x 50 µl were transferred to new 1.5ml microcentrifuge tubes, while the rest was used to elute the immunoprecipitated protein from the beads. The supernatant was removed from the tubes for the activity assay using a magnetic rack. In the next step, the beads were covered with 20 µl Hunt buffer + inhibitors and incubated with 4µl ^{3}H-labeled histones for 4-5h at 30°C while shaking at 300 rpm. For the input sample, 20 µg of whole protein extract was used. To stop the reaction, 35µl Histone stop solution and 800µl Ethyl acetate were added to the samples. Following, the tubes were vortexed for at least 15 seconds and centrifuged for 4 minutes at 10000rpm in a swing out bucket. During this process, two phases emerged. From the upper organic phase 600µl were transferred to a tube filled up with 3 ml Scintillation solution and gently mixed by inverting. The efficiency of acetyl-group removal was measured as counts per minute in a scintillation counter.

Histone stop solution

1 M HCl

0.4 M Sodium acetate

Scintillation solution

5 g/l PPO (2,5-Diphenyloxazole)

0.5 g/l POPOP (1,4-bis(5-phenyloxazol-2-yl) benzene

Filled up with toluene

3. Results

3.1 Analysis of HAP1 cell lines expressing acetyl HDAC1 mutants

3.1.1 Mutation of K412 has no effect on HDAC1 activity

First, we immunoprecipitated FLAG-HDAC1 from the whole protein extracts obtained from each cell line. Our aim was to investigate if the acetylation state of lysine 412 on HDAC1, which is mimicked by K412Q or prevented by K412R, influences the stability of the protein. Via Western blot analysis we confirmed the presence of immunoprecipitated FLAG-HDAC1 protein (Figure 6). We used one third of the precipitate to measure the deacetylase activity of HDAC1 in the different mutants. The histone deacetylase activity was measured as counts per minute in a scintillation counter using ^{3}H-acetate labeled histones as a substrate (Figure7).

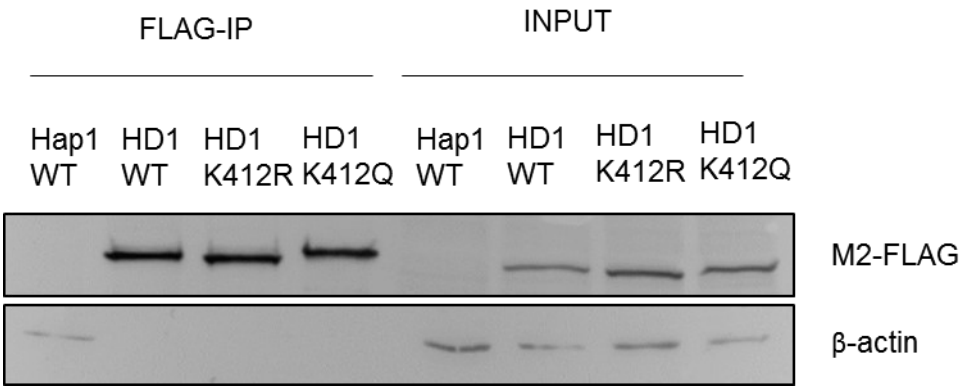

Figure 6. Western Blot analysis of immunoprecipitated HDAC1 acetyl mutants. FLAG-tagged HDAC1 WT, K412R and K412Q were immunoprecipitated using anti-FLAG M2 beads from whole-cell extracts. Two thirds of the immunoprecipitate was used for Western blot analysis while one third was utilized to measure HDAC1 activity.

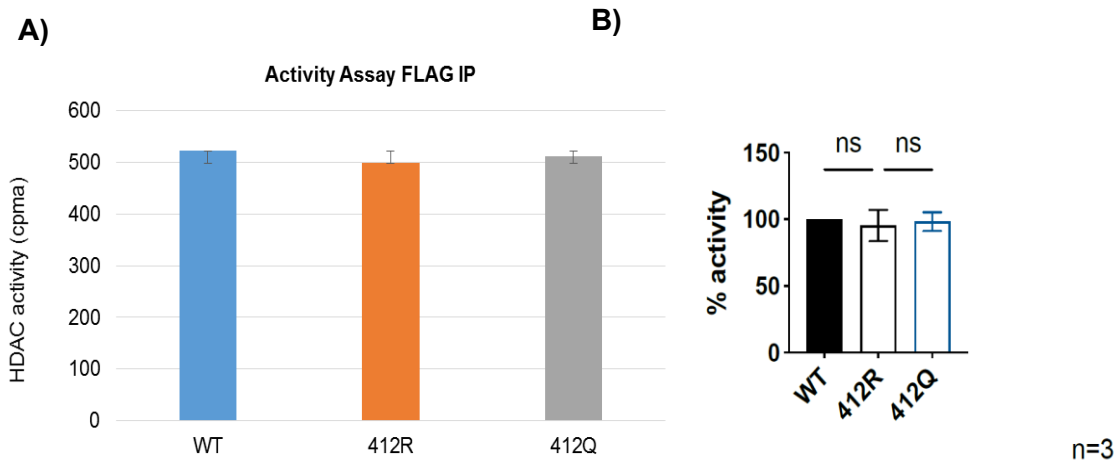

Figure 7. Activity Assay of FLAG Immunoprecipitates. HDAC1 proteins were immunoprecipitated from the protein extracts of each cell line using FLAG M2 magnetic beads. One-third of the immunoprecipitated protein was used to measure HDAC activity as counts per minute using 3H-acetate labeled histones as a substrate (CPM). The assays were performed in biological triplicates. **A)** HDAC activity as counts per minute (cpma reflects the amount of acetate groups released by HDACs from histone proteins within the 4 hours). **B)** HDAC activity depicted in percent compared to wildtype HDAC1 activity set to 100%.

Figure 6 shows that the intensity of the FLAG signal is relatively similar, indicating that comparable amounts of protein were precipitated. We assumed that the reduced binding of HDAC1 K412R mutant to the co-repressors (which is shown in more detail in 3.2.1, Figure 9A) would negatively affect its deacetylase activity. However, we could not prove any significant reduction in the deacetylase activity of the HDAC1 K412R mutant compared to WT (Figure 7). In summary, the activity assay showed no significant difference in HDAC1 activity between WT and HDAC1 K412R and HDAC1 K412Q mutants.

3.1.2 Mutation of K412 has no effect on HDAC1 stability

To further analyze the effect of K412R acetylation on HDAC1 function we followed the protein stability in the mutants expressing different isoforms of HDAC1 using cycloheximide time course experiment. Cycloheximide is a translational inhibitor, causing the cells to stop producing new protein after incubation with the chemical. Degradation of HDAC1 protein was followed using Flow cytometry. The experiment was performed in biological duplicates. Figure 8 shows that there is no significant difference in the protein stability of HDAC1 WT compared to HDAC1 K412R and HDAC1 K412Q.

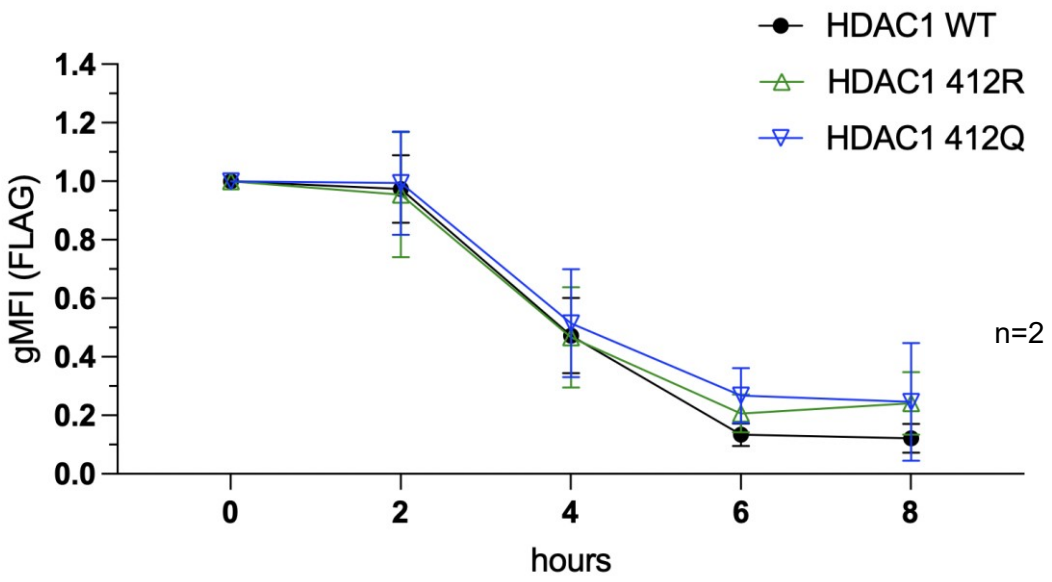

Figure 8. Cycloheximide time course experiment. The cells were treated with 300µg/ml of cycloheximide dissolved in DMSO. Samples were collected 0h, 2h, 4h, 6h and 8h after treatment. FLAG signal was measured using flow cytometry.

After incubating the cells with cycloheximide, a time-dependent decrease in the amount of FLAG-HDAC1 protein can be seen in all mutants and the WT. However, we did not detect a significant difference in the stability of the HDAC1 acetyl mutants compared to HDAC1 WT.

Taken together, our biochemical assays did not reveal any significant differences in the characteristics of the HDAC1 acetyl mutants compared to WT. Neither catalytic activity nor protein stability were affected by mutating the lysine 412 locus into arginine (412R) or glutamine (412Q).

3.2 Interactome of HDAC1 acetyl mutants

3.2.1 Investigation via FLAG immunoprecipitation

To execute its deacetylase activity HDAC1 needs to be incorporated into co-repressor complexes such as the Mi-2/NuRD complex, CoREST complex or SIN3A complex. In these experiments we immunoprecipitated FLAG-tagged HDAC1 protein isoforms to analyze the binding affinity to its interaction partners. In the experimental approach we intended to precipitate an identical amount of protein for each isoform. If necessary the amount of input protein extract was adapted in consonance with HDAC1 abundance. The proteins were separated by SDS-PAGE and transferred onto a nitrocellulose membrane via the wet transfer

method. Presence of the protein was analyzed by immunodetection using the corresponding antibodies specific for the FLAG tag, CoREST, MTA2, HDAC2 and HDAC1. For quantification ImageJ software was utilized, the measured values for each interaction partner were normalized to the FLAG signal.

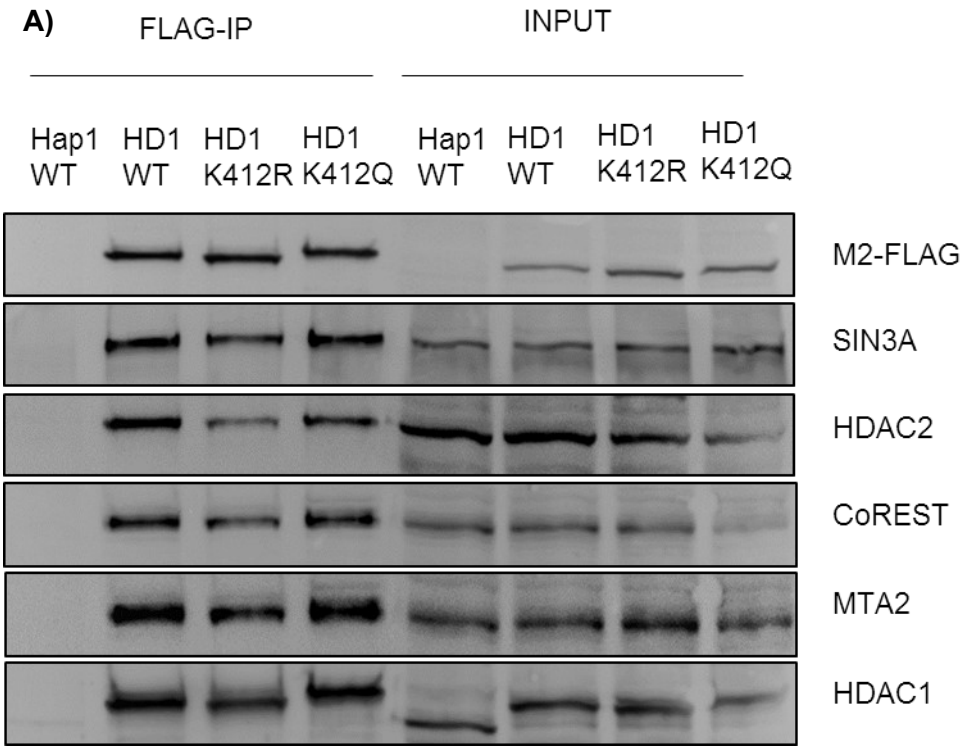

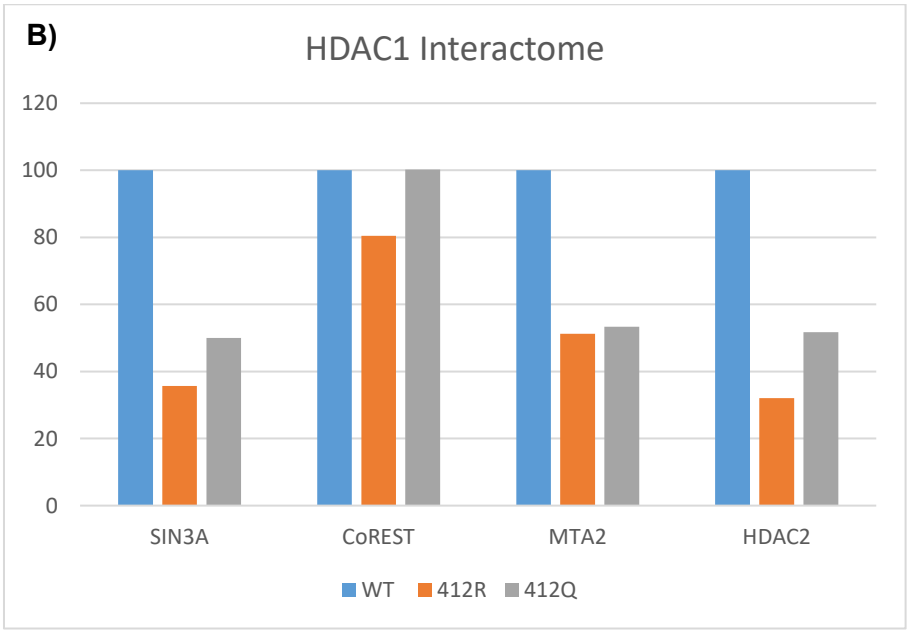

Figure 9. Western Blot analysis of immunoprecipitated HDAC1 acetyl mutant proteins. FLAG-tagged HDAC1 WT, K412R and K412Q were immunoprecipitated using anti-FLAG M2 beads from whole-cell extracts. **A)** One-third of the immunoprecipitate was separated by 10% SDS-PAGE and analyzed via Western blot using indicated antibodies. As input, whole-protein

extracts were used. HAP1 WT was included as a negative control. **B)** Western blot signals of co-immunoprecipitated co-repressor proteins were quantified using ImageJ and normalized to the measured FLAG signal. The values are represented relative to HDAC1 WT.

The results we obtained, suggest that the immunoprecipitated amount of FLAG-tagged protein is relatively equal for wildtype HDAC1 and all mutants. This was also confirmed by the signal of the HDAC1 SAT208 antibody, which is comparable for all HDAC1 isoforms. Regarding the signal of SIN3A and HDAC2 antibody it seems to be less in 412R mutant compared to the other mutants (Figure 9A). Western blot signals of co-immunoprecipitated co-repressor proteins were quantified with ImageJ (Figure 9B). These results suggest a reduced binding of HDAC1 K412R mutant to the co-repressor HDAC2. However, there appears to be no effect on the activity of the mutant (Figure 7).
To further investigate these findings, we isolated HDAC1 protein by FLAG-IP from nuclear extracts and performed mass spectrometry analysis as well as specific SIN3A and HDAC2 co immunoprecipitation experiments.

3.2.2 Investigation via mass spectrometry upon FLAG-IP from nuclear extracts

In this unbiased approach, we determined the protein interactome of HDAC1 acetyl mutants in HAP cells via mass spectrometry. Before proceeding with mass spectrometry we performed FLAG immunoprecipitation with nuclear proteins. HDAC1 is a nuclear protein, but under certain conditions it can also be found in the cytosol. Class I HDACs are mostly present in the nucleus, while class II HDACs fluctuate between the cytosol and the nucleus. In both cases HDACs carry out important cellular functions such as apoptosis, cell cycle regulation and transcriptional control. In the cytoplasm HDACs regulate the acetylation of tubulin present in the cytoplasm (Kong et al., 2013). However, in HAP1 cells HDAC1 shows predominant nuclear localization (master thesis Natalija Cvetcovic, 2022). Following the nuclear extraction protocol previous to the pulldown resulted in a cleaner fraction and the absence of cytosolic factors which might contaminate the HDAC1 interactome. This protocol (Winter et al. 2013), involves the use of a high salt containing nuclear extraction buffer and is therefore called “high salt extraction” (HSE) method. With this method we were able to obtain a considerable high amount of nuclear extract which was used for FLAG immunoprecipitation. Input, pulldown and supernatant were analyzed via Western blot (Figure 10). The mass spectrometry approaches should serve to determine potential differences in the interactomes of wildtype HDAC1 and the distinct acetyl mutants. In this study we focus on the impact of the 412R mutation which prevents K412 acetylation. After performing the pulldowns the samples were further processed and analyzed by the group of Markus Hartl (Mass spectrometry facility MPL). First, the proteins

were separated from the beads via a tryptic digest to obtain small peptide fragments. In the following step the fragments were separated using a nano HPLC system which is coupled to an Orbitrap mass spectrometer with a nanospray ionisation source. Subsequently, the found peptides were compared with the Uniport database. An LFQ-algorithm was taken into account to process the protein intensities obtained by mass spectrometry. In an additional step, contaminations were eliminated from the precipitates and low-quality hits were removed.

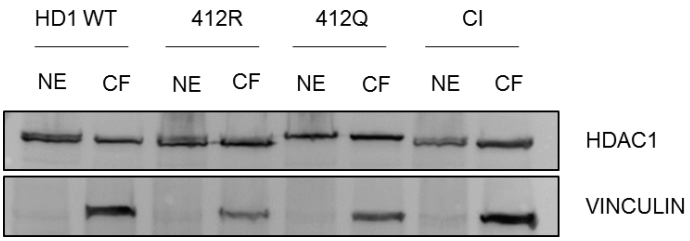

Figure 10. Western Blot analysis of nuclear extracts prepared with the HSE method. NE (Nuclear Extract), CF (Cytosolic Fraction). One fifth of the extracts was used for Western Blot analysis to validate the efficiency of the nuclear extracts.

In previous studies our lab has generated cell lines expressing catalytically inactive (CI) HDAC1 mutant. In this experiment this mutant was taken into account, additionally. CI mutants contain the point mutation at H141A in their catalytic center which makes them catalytically inactive but does not prevent the enzymes to fulfil structural functions (Hess, Moos et al., 2022). Thus, CI mutants can mimic HDAC1 inhibition. Vcelkova and Reiter proposed that HDAC1 itself is a potential non-histone target of HDAC1. Suggesting that in the HDAC1 CI mutant, HDAC1 itself is present in a hyperacetylated state (Figure 5). Which in turn makes the CI mutant an interesting alternative to investigate, if the acetylation of HDAC1, has an effect on its interaction with other proteins.

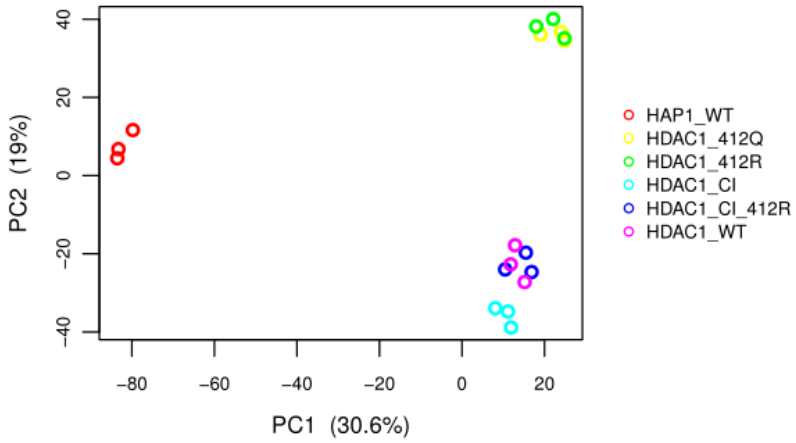

Figure 11. Principal component analysis after imputation of missing values. This PCA plot shows clustering of triplicates of HAP WT, HDAC1 WT, K412R, K412Q, HDAC1 CI and HDAC1 CI K412R samples based on their similarity.

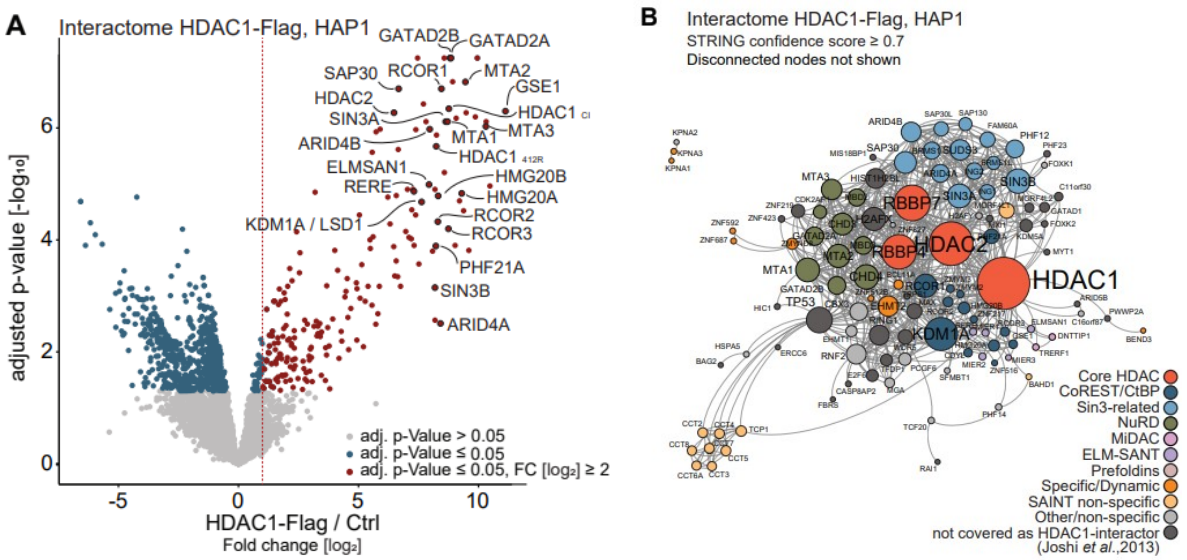

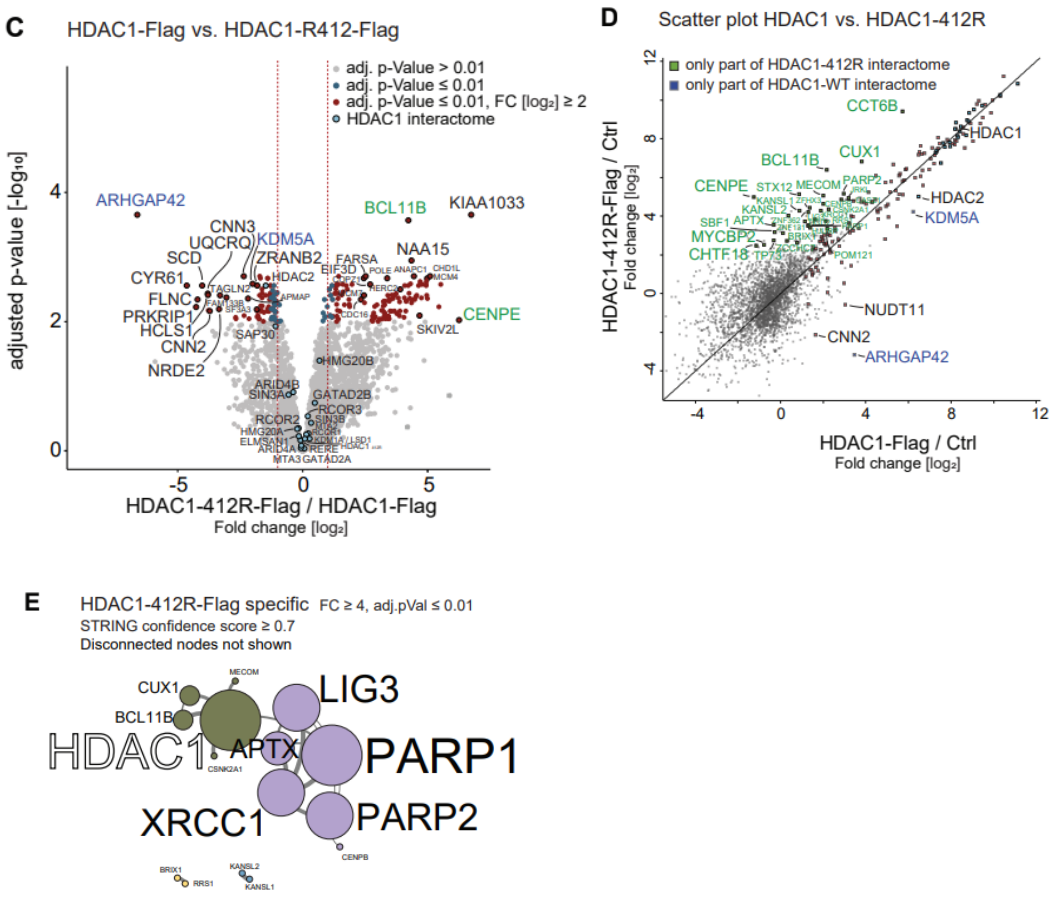

Figure 12. HDAC1 WT and 412R Interactomes. A) HDAC1 WT Interactome compared to HAP1 control. **B)** Change in Interactome due to K412R mutation. **C)** Protein network based on Panel A. **D)** Comparative analysis of HDAC1 WT and 412R Interactomes. Proteins indicated in green are found in 412R Interactome but not in HDAC1 WT Interactome. **E)** Protein network based on proteins only found in 412R Interactome (green in Panel D). Proteins indicated in purple are involved in DNA repair.

The PCA plot (Figure 11) shows that biological triplicates for samples of the different genotypes cluster together demonstrating the high quality of the mass spectrometry analysis. HAP WT control shows the least similar behavior compared to the HDAC1 acetyl mutants and therefore clusters on the opposite site of the plot. Interestingly, HDAC1 K412Q mutant (yellow) clusters together with HDAC1 K412R mutant (green) which suggests that they display a similar behavior regarding their interactomes. The other interactomes depicted in Figure 11 (HDAC1 CI and HDAC1 CI K412R) will be analyzed in future studies.

In Figure 12 the interactomes of the HDAC1 acetyl mutants are depicted in more detail. In panel A the HDAC1 WT Interactome is compared to HAP1 control. Some of the affected proteins are known to be part of the co-repressor complexes SIN3A, NURD and CoREST. The most interesting upregulated proteins are MBD3, GATAD2B, GATAD2A, SUDS3, CHD4, MTA2, RCOR1, SAP30, RBBP7, GSE1, BRMS1L, HDAC2, SAP130, MTA1, SIN3A, FOXK2,

RREB1, BRMS1, MTA3, MBD2, SAP30L, FAM60A, HMG20B, BEND7, RCOR2, RCOR3, FOXK1, ZNF516, ZNF592, GATAD1, SALL1, SIN3B and BEND3.

The change in the interactome due to K412R mutation is also depicted in Figure 12 (Panel B). Most of the proteins upregulated due to K412R mutation are not known to be part of the co-repressor complexes of HDAC1 and don't play a role in protein acetylation. To name some of the top hits: KIAA1033, BCL11B, NAA15, CHD1L, ANAPC1, FARSA, POLE, EIF3D, MCM4, EPB41L3, NIPBL. An exception is PHF20, it is upregulated due to K412R mutation and plays a role during protein acetylation. The FLAG immunoprecipitation experiments suggest a reduced binding of HDAC1 K412R mutant to the co-repressors complexes (Figure 9), this could not be confirmed by the interactome data of the mass spectrometric analysis. Proteins that are downregulated due to K412R mutation are ARHGAP42, CNN3, BOLA2, HMGA2, KDM5A, CYR61, SCD, and ZRANB2. However SIN3A does not appear to be affected upon K412R mutation. However, a trend of reduced interaction of HDAC2 with the K412R mutant in comparison to HDAC1 WT can be observed. Proteins that only part of the K412R interactome (Figure 12, panel D) are CUX1, BCL11B, CENPE, MYCBP2, CHTF18, SBF1, KANSL2, MECOM, STX12, APTX, KANSL1. A protein network based on proteins only found in 412R interactome is depicted in panel E, proteins indicated in purple are involved in DNA damage repair.

3.2.3 HDAC1 K412R interaction with SIN3A and HDAC2

Analysis of the interactome by FLAG immunoprecipitation indicated a decrease in the interaction of HDAC1 with HDAC2 in the HDAC1 K412R mutant when compared to HDAC1 WT protein (Figure 9). We also saw a slight reduction in the interaction of HDAC1 with SIN3A in the HDAC1 K412R mutant when compared to HDAC1 WT. Due to this findings we wanted to investigate the behavior of HDAC2 and SIN3A in the K412R mutant in more detail. Therefore, HDAC2 co-immunoprecipitation as well as SIN3A co-immunoprecipitation experiments were performed. Part of the immunoprecipitate was eluted with SDS and analyzed on Western blots. The other part was used for the activity assay using ^{3}H-acetate labeled histones.

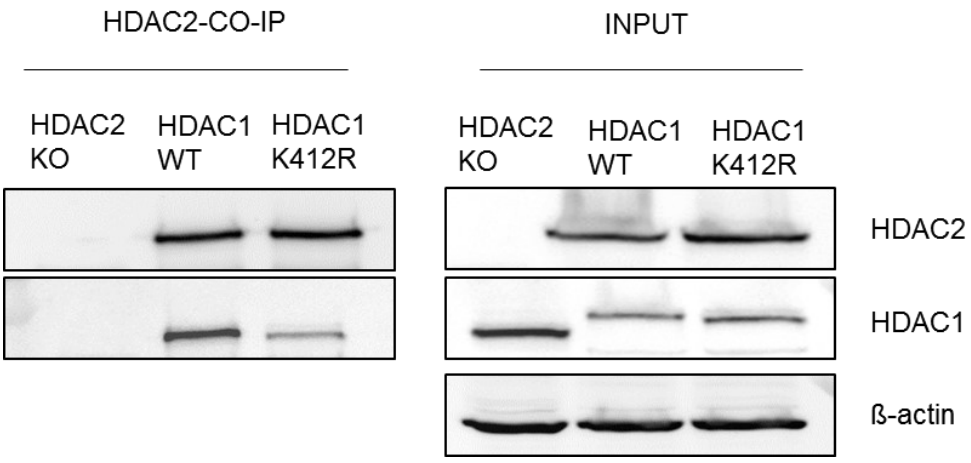

Figure 13. Western Blot analysis of HDAC2 co-immunoprecipitation. Two thirds of the immunoprecipitated HDAC2 protein was eluted and analyzed by Western blotting with indicated antibodies. The HDAC2 KO cell line was included as negative control. For input 20µg of the respective whole protein extracts were used.

In the Western blot analysis (Figure 13) it was confirmed that comparable amounts of HDAC2 protein were precipitated from HDAC1 WT and HDAC1 412R extracts. Additionally, protein extracts of HDAC2 KO cell line were, were loaded on a gel as negative control. However, the signal of co-precipitated HDAC1 protein was weaker in the HDAC1 K412R mutant compared to HDAC1 WT although the same amount of HDAC2 protein was precipitated. This would again suggest that the K412R acetyl mutant HDAC1 interacts less with HDAC2 than the wildtype enzyme. Data from the mass spectrometry analysis also show a trend to reduced interaction of HDAC2 with the K412R mutant in comparison to HDAC1 WT (Figure 12).

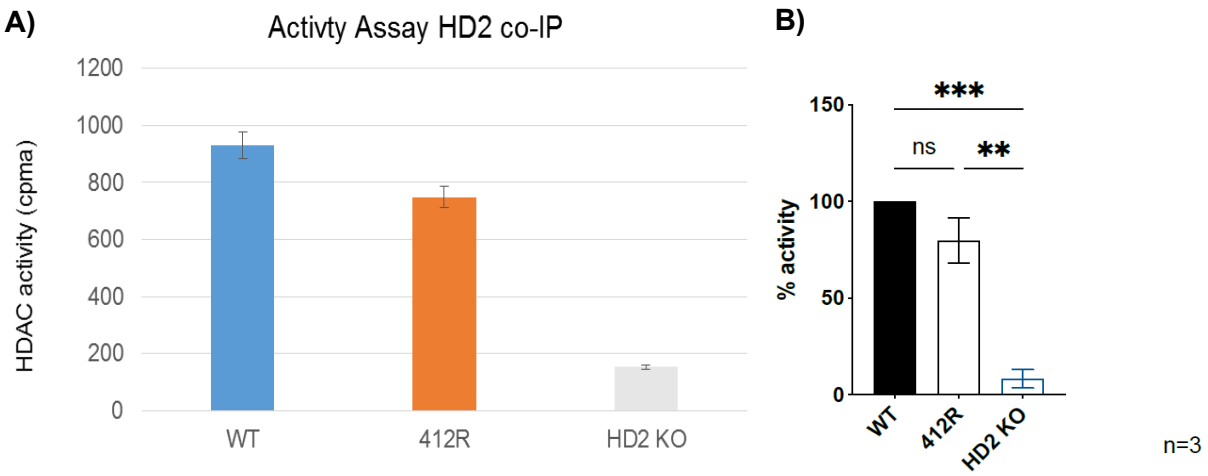

Figure 14. Activity Assay of HDAC2 Immunoprecipitates. HDAC2 proteins were immunoprecipitated from the protein extracts of each cell line using magnetic beads and HDAC2 antibody. One-third of the immunoprecipitated protein was used to measure HDAC activity as counts per minute using 3H-acetate labeled histones as a substrate (CPM). The

assays was performed in biological triplicates. **A)** Representative data of one of the triplicates (cpma reflects the amount of acetate groups released by HDACs from histone proteins within the 4 hours). **B)** Relative HDAC activity in percent compared to wildtype set to 100%.

The activity assay revealed a slight difference between HDAC1 WT and HDAC1 K412R (Figure 14 A). However this tendency could not reach a significant statistical difference (Figure 14 B). Although, Western blot analysis suggests that in the K412R mutant HDAC1 interacts less with HDAC2, it doesn't seem like that the HDAC activity is significantly decreased in the mutant when compared to HDAC1 WT.

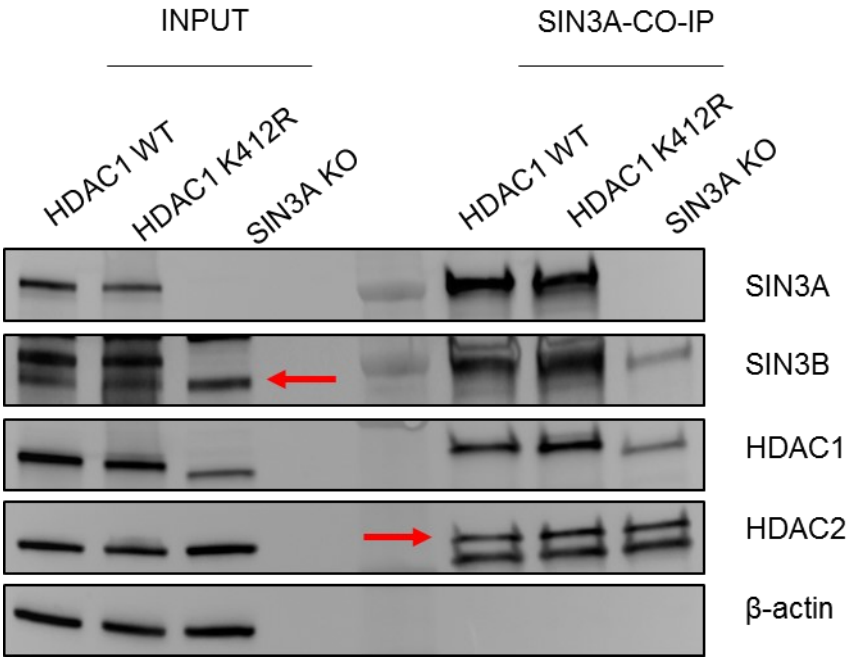

Figure 15. Western Blot analysis of SIN3A co-immunoprecipitation. Two thirds of the immunoprecipitated SIN3A protein was eluted from the beads and analyzed by Western blotting with indicated antibodies. For input 20µg of the respective whole protein extracts were used. Protein extracts of SIN3A KO cells were loaded as a negative control.

Analysis of the immunoprecipitates via Western blot verified efficient precipitation of SIN3A and that similar amounts of SIN3A protein was precipitated from HDAC1 WT and HDAC1 K412R mutant extracts (Figure 15). HDAC1 and HDAC2 signal appear to be stronger in HDAC1 K412R mutant compared to HDAC1 WT in contrast to the data of the FLAG IP experiments (3.2.2, Figure 9A) which initially suggested weaker interaction between HDAC1 and SIN3A in the HDAC1 K412R mutant. Surprisingly, HDAC1 and HDAC2 was found in the immunoprecipitate from the negative control, the SIN3A KO cell line. This might be due to a cross-reaction of the SIN3A antibody with the SIN3A homologous protein SIN3B, which was

present in the SIN3A KO immunoprecipitate. The presence of SIN3B in the SIN3A immunoprecipitates could also obscure the quantitative analysis of HDAC1/SIN3A interaction.

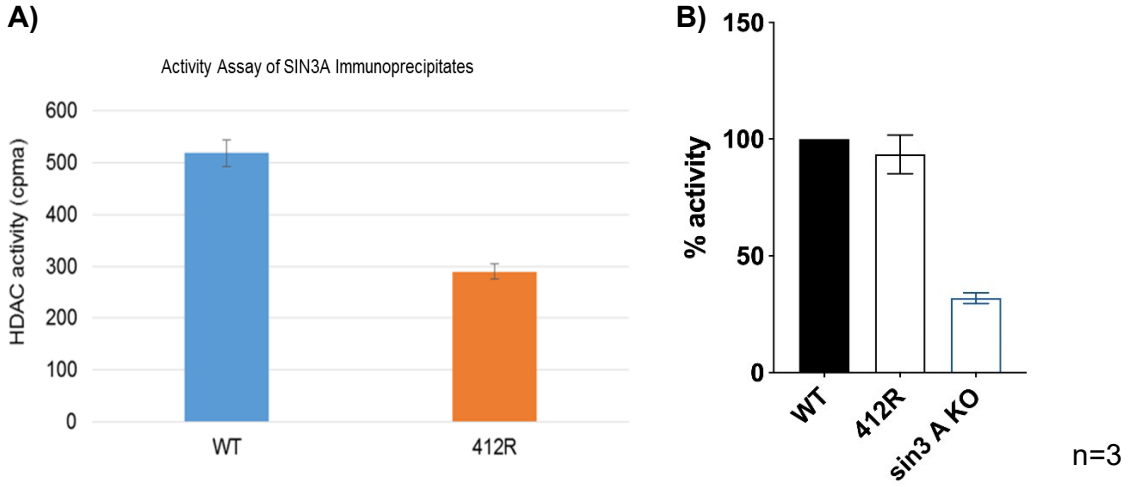

Figure 16. Activity Assay of SIN3A Immunoprecipitates. SIN3A proteins were immunoprecipitated from the protein extracts of each cell line using magnetic beads and Anti-SIN3A antibody. One-third of the immunoprecipitated protein was used to measure SIN3A activity as counts per minute using 3H-acetate labeled histones as a substrate (CPM). The assays was performed in biological triplicates. **A)** HDAC activity as counts per minute, representative figure of one of the biological tripilactes (cpma reflects the amount of acetate groups released by HDACs from histone proteins within the 4 hours). **B)** Relative HDAC activity in percent compared to wildtype set to 100%.

The HDAC activity assay of the SIN3A IP shows no significant difference between HDAC1 WT and HDAC1 K412R. The activity of HDAC1 appears to be reletaivley equal in both cell lines. In summary, SIN3A immunoprecipiation experiments do not confirm weaker interaction between HDAC1 and SIN3A in the HDAC1 K412R mutant as previously indicated in the FLAG IPs.

All in all, it can be concluded from the data obtained in the FLAG immunoprecipitation experiments (Figure 9A) and the HDAC2 co immunoprecipitation experiments (Figure 13), that the interaction between HDAC1 and HDAC2 is somehow reduced in the HDAC1 K412R mutant in which K412 of HDAC1 is resistent to acetylation. On the other hand, data obtained from the SIN3A co immunoprecipitation experiments do not correspond with the data from FLAG immunoprecipitation experiments. Thus, we can not say for sure if the same is true for the SIN3A co-repressor complex and its interaction with HDAC1 in the HDAC1 K412R mutant. Regarding the results from the mass spectrometry analysis, which do not show a downregulation of the SIN3A protein in HDAC1 K412R mutant when compared to HDAC1 WT, it can rather be assumed that the interaction of SIN3A is not significantly affected in the mutant (Figure 12, panel D).

3.3 Production of monoclonal antibody against acetylated K412

Another goal of the project was to produce and characterize a monoclonal antibody specifically directed against acetylated lysine K412 on HDAC1. Such an antibody could later be used to identify HDAC1 which is acetylated at K412. The idea was to generate an antibody which could find application in several approaches such as Western blot detection, immunoprecipitation or Flow cytometry. Regarding our project, the antibody could be validated by using HDAC1 mutants. By successfully producing the antibody it could be used to recognize acetylated K412 in the HDAC1 wildtype protein but not in the K412R mutant. Furthermore, the CI mutant should display a very strong signal when incubated with the antibody, since in this mutant HDAC1 is catalytically inactive and the protein itself is therefore present in a hyperacetylated state (Hess, Moos et al, 2022). In contrast, HDAC1 CI K412R mutant should not be able to be recognized by the antibody since in this case K412 is resistant to acetylation. The generation of the antibody was performed by Stefan Schüchner at the MPL Monoclonal Antibody facility.

3.3.1 Serum screen of immunized mice via ELISA

In the first step of producing the antibody, mice were immunized with the peptide encompassing amino acids 408/409 to 414/416 with acetylated K412, which was linked to keyhole limpet hemocyanin (KLH) via either the C-terminus or the N-terminus of the peptide. After immunization serum was isolated and analyzed via ELISA (Figure 17). In case of the mice which were injected with the N-terminal linked peptide mouse M3 showed the best response while in case of the C-terminal injection mouse M1 and M3 were promising targets.

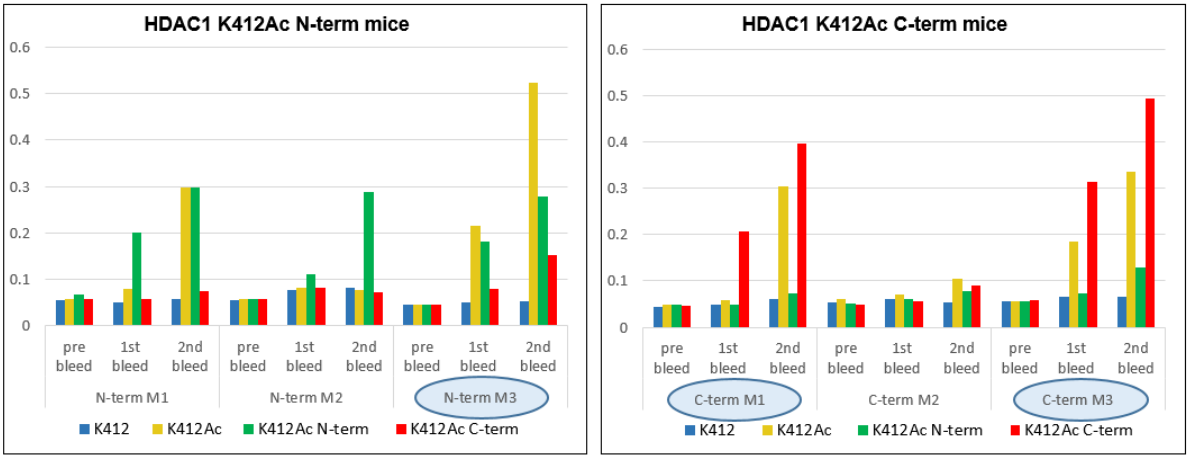

K412: **Ac-SICSSDKRIACEEEFSDSEE-NH2**
K412Ac: **Ac-SICSSDK(Ac)RIACEEEFSDSEE-NH2**
K412Ac N-term: **Ac-CSSDK(Ac)RIA-NH2**
K412Ac C-term: **Ac-SSDK(Ac)RIAC-NH2**

Figure 17. HDAC1 K412Ac Serum Screen (ELISA). The acetylated peptides were coupled via naturally occurring cysteines in the HDAC1 sequence to KLH. There is an N-terminal as well as a C-terminal cysteine near to K412. Three mice each were injected with the HDAC1 K412Ac N-terminal linked peptide and the C-terminal linked peptide. Positive mice were identified by ELISA screen with the indicated peptides. (Figure kindly provided by Stefan Schüchner).

The specificity of the antibody was additionally tested via Western blot using whole cell extracts of HDAC1 WT and HDAC1 CI cells (Figure 18). In the whole cell extract no signal could be detected when the membrane was incubated with the sera obtained from the mice that showed the best response in the ELISA screen (N-term M3 and C-term M3). Hence, we decided to enrich for acetylated proteins by performing acetyl-lysine immunoprecipitation experiments.

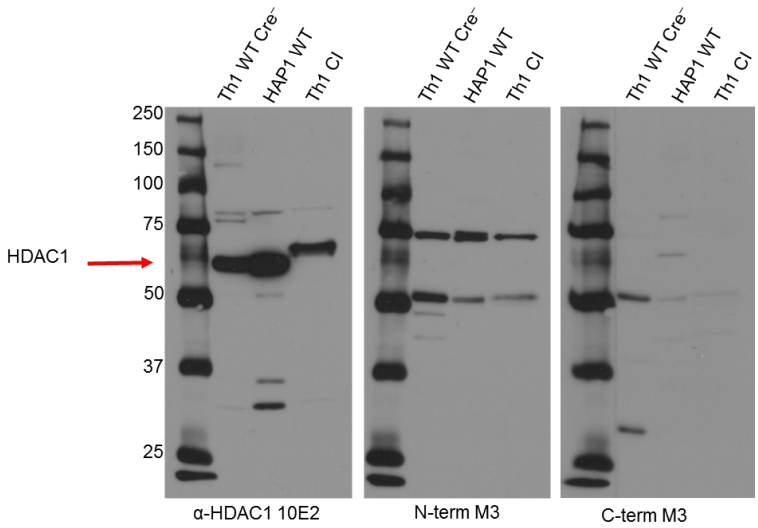

Figure 18. Western blot analysis of whole cell extracts. A serum screen was performed on whole cell lysates. Replica membranes were incubated with HDAC1 10E2 antibody as positive control (band for HDAC1 is indicated by the red arrow) or sera obtained from N-term M3 and C-term M3. In the case of the sera no signal was detected at the height of HDAC1.

3.3.2 Acetyl-lysine immunoprecipitation to enrich for acetylated protein

In contrast to histones, non-histone acetylation target proteins show only a very low level of acetylation in mammalian cells (Hansen et al., 2019). To better be able to detect acetylated HDAC1 we enriched for acetylated proteins via acetyl-lysine immunoprecipitation for the antibody validation. The precipitates were used to verify the presence and specificity of

antibodies in the sera, cell lysates and supernatants. We expected that the signal for acetylated HDAC1 should be weaker in the double mutant (HDAC1 CI 412R) compared to the CI mutant, since lysine residue 412 should be resistant to acetylation in the HDAC1 CI 412R mutant.

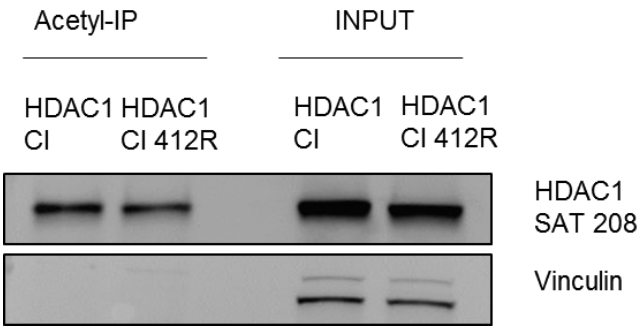

Figure 19. Western blot analysis of Acetyl-Lysine IP. Acetylated protein was immunoprecipitated using acetyl-lysine beads from whole cell extracts. Part of the immunoprecipitate was separated by 10% SDS-PAGE and analyzed via Western blot using indicated antibodies.

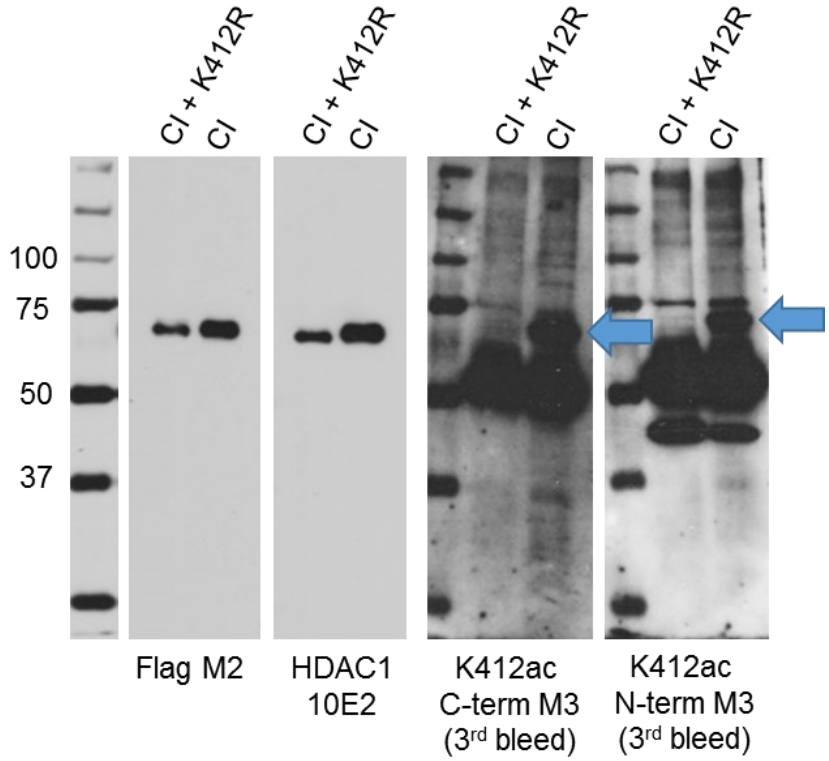

Figure 20. Western blot analysis of acetyl-lysine IP using mouse sera. We performed a serum screen using acetylated proteins isolated by the previously performed Acetyl-IPs for Western blot analysis. In this case K412ac C-term M3 (3rd bleed) and K412ac N-term M3 (3rd bleed) were tested. Both sera showed a signal at the height of HDAC1 (indicated with blue arrow) in the HDAC1 CI acetyl IP but not in the HDAC1 CI K412R mutant acetyl IP.

We successfully precipitated acetylated proteins from both HDAC1 CI and HDAC1 CI K412R cell extracts (Figure 19). The precipitates were then used to validate the presence of the antibody against acetylated K412 in the mouse sera chosen from the ELISA Screen. The results obtained from these Western blot analysis, looked very promising. When using sera from the N-terminal M3 mouse and the C-terminal M3 mouse, we only obtained a signal at the height of HDAC1 in the HDAC1 CI mutant but not in the HDAC1 CI K412R mutant (Figure 20), which is supposed to be resistant to acetylation on K412. These findings would propose that the antibodies present in these sera specifically recognize acetylated K412 on HDAC1.

3.3.3 Verification of monoclonal antibody on acetyl – lysine immunoprecipitates via Western blot analysis

Based on the Western blot screen with the acetyl-IPs, the sera of N-terminal M3 mouse and C-terminal M3 mouse were promising. To proceed with the development of the monoclonal HDAC1 K412ac antibody these mice were sacrificed after being exposed to a booster immunization. In the next steps spleen cells were fused with myeloma cells. Hybrid cells were selected and separated to allow them to proliferate into clones. The clones derived from mouse C-terminal M3 are further referred to as 8D7 for the polyclonal supernatant and 8D7-E4 for the monoclonal supernatant. Since the results from Figure 20 looked very promising we expected similar results in the continuing experiments. The polyclonal supernatant 8D7 gave strong signals for HDAC1 CI but not for HDAC1 CI 412R (Figure 21). However, FLAG as well as HDAC1 10E2 antibody evaluation indicated that much more protein was precipitated in HDAC1 CI mutant compared to HDAC1 CI 412R mutant (Figure 21).

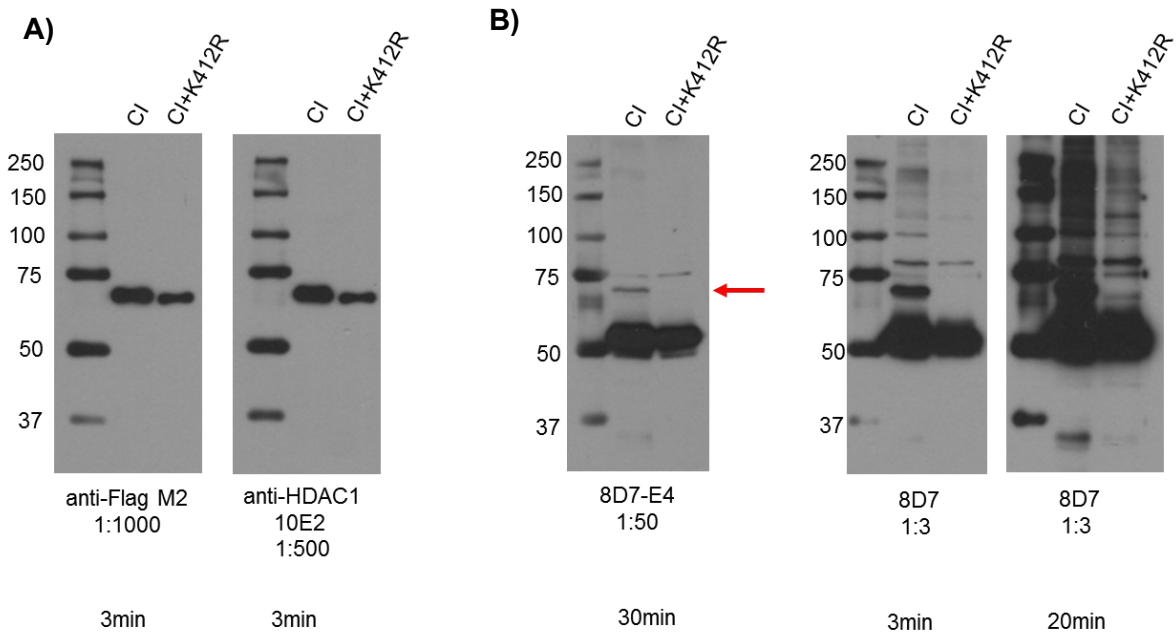

Figure 21. Western blot analysis of acetyl-lysine IP using mixed and single cell clones. **A)** Acetyl-lysine immunoprecipitates were separated by 10% SDS-PAGE and analyzed via Western blot. FLAG M2 and HDAC1 10E2 antibodies were used for evaluation, in both cases the signal is much stronger in the HDAC1 CI mutant. **B)** Polyclonal 8D7 as well as monoclonal 8D7-E4 supernatants were tested for recognition of acetylated K412. Exposure time was increased from three to twenty minutes.

Due to the unequal amount of acetylated protein loaded on the Western blot we cannot trust the results from the first screen of the supernatant. Therefore, we attempted to adjust the amount of precipitate loaded on the gel.

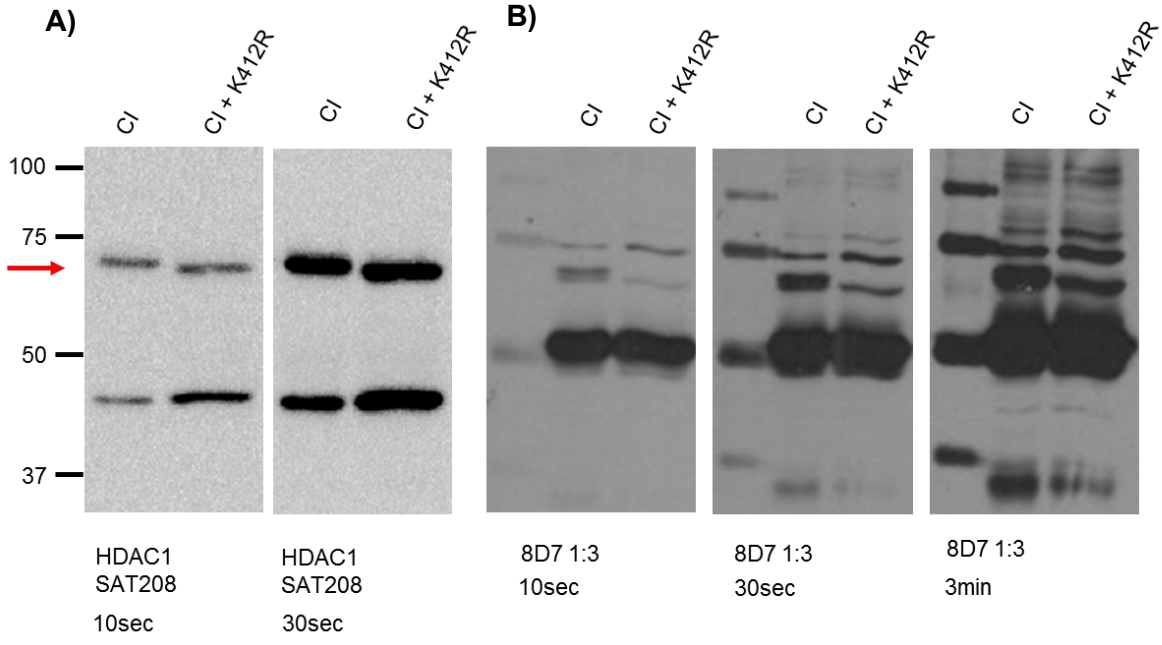

Figure 22. Western blot analysis of acetyl-lysine IP using polyclonal supernatants. A) Adjusted amount of HDAC1 using HDAC1 SAT208 antibody. (Signal for HDAC1 is indicated by the red arrow). Exposure time was increased from ten to thirty seconds. **B)** Retest of clone 8D7 on acetyl immunoprecipitates. Exposure time was increased from ten to thirty seconds, up to three minutes.

After all, we managed to adjust the amount of protein extract used according to the HDAC1 protein abundance. Figure 22 shows that comparable amounts of HDAC1 are present for both isoforms. However, when incubating with supernatant 8D7 we observed an additional signal at the height of HDAC1 for both mutants (Figure 22). In addition, the monoclonal 8D7-E4 supernatant showed a much weaker signal in the HDAC1 CI 412R IP (Figure 21 B).

Taken together, we cannot fully trust that the supernatant 8D7 has the specificity to distinguish between acetylated and deacetylated K412 on HDAC1. Therefore we decided to go back one step and perform the single cell dilution with another polyclonal cell mixture (5G12).

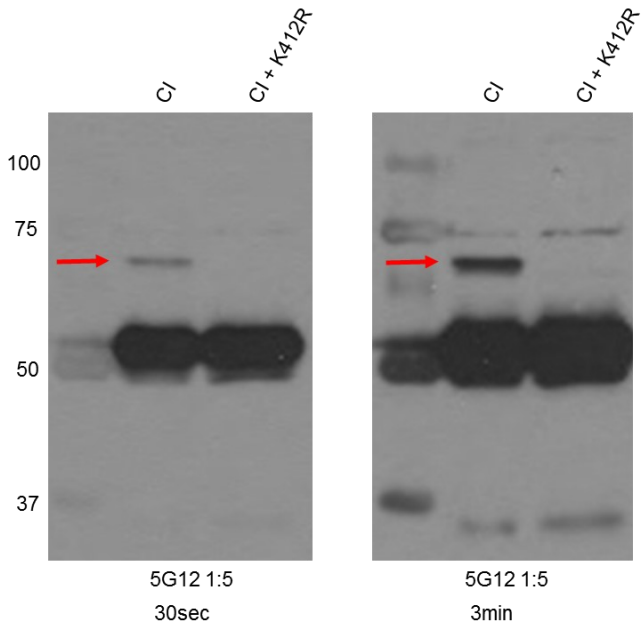

Figure 23. Western blot analysis of acetyl-lysine IP using new polyclonal supernatant of 5G12. Acetyl-lysine immunoprecipitates of HDAC1 CI and HDAC1 CI K412R mutants were separated by 10% SDS-PAGE and analyzed via Western blot. The mixed clone 5G12 was tested for recognition of acetylated K412. The HDAC1 signal is indicated by the red arrow. Exposure time was increased from 30 seconds up to 3 minutes.

Western blot analysis of the new polyclonal supernatant 5G12 showed a signal in the HDAC1 CI mutant but not in the HDAC1 CI K412R mutant. Hence, with the new clone (5G12) we were eventually able to show the specificity of the antibody.

In a further step we performed a single cell dilution with the successfully tested mixed clone 5G12 to obtain a new monoclonal supernatant. The single clone 5G12-3H3-D8 was then used to test if we get a signal for acetylated K412 on HDAC1 when incubating the supernatant on FLAG-HDAC1 immunoprecipitates.

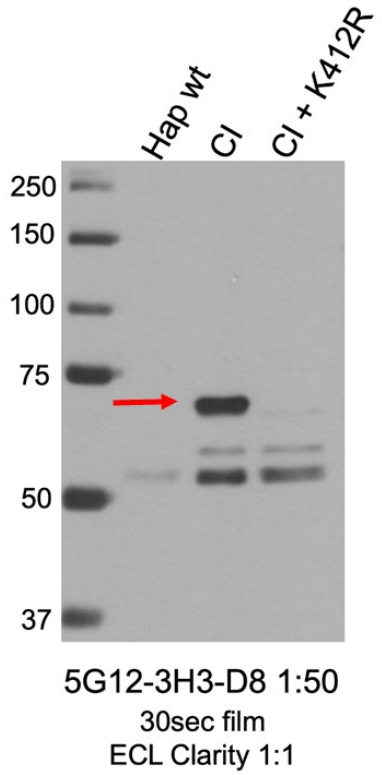

Figure 24. Western blot analysis of FLAG immunoprecipitates using monoclonal supernatant 5G12-3H3-D8. FLAG immunoprecipitates of HAP WT, HDAC1 CI and HDAC1 CI K412R mutants were separated by 10% SDS-PAGE and analyzed via Western blot. The single clone 5G12-3H3-D8 was tested for recognition of acetylated K412. Band for HDAC1 is indicated by the red arrow. Exposure time was 30 seconds.

Western blot analysis of the single clone 5G12-3H3-D8 showed a signal in the HDAC1 CI mutant but not in the FLAG-IPs of HAP1 WT cells (no acetylated K412 HDAC1 signal) and HDAC1 CI K412R mutant cells, confirming the specificity of the monoclonal antibody present in the supernatant, which only recognizes acetylated K412 on HDAC1.

4. Discussion and outlook

Histone acetylation impacts chromatin-associated processes such as transcription, replication, DNA compaction and DNA repair and is controlled by the antagonistic activity of HATs and HDACs (Turner, 1991). Thus, these enzymes play an important role in gene regulation. More accurately, HDAC activity is mainly linked to repression and silencing of genes while HATs are primarily related to active chromatin (Marmorstein & Zhou, 2014). In many different types of cancers, HATs and HDACs are known to be altered in structure and function. Hence, understanding the detailed structure and function of HDACs has become crucial part in terms of developing specific anti-cancer drugs (Timmermann et al., 2001). Some HDAC inhibitors (HDACi) have already been investigated for their potential in cancer treatment. However, the HDACis that are currently in use show almost no specificity and are linked to various undesired side effects (Botrugno et al., 2012). Therefore it is essential to develop more specific HDACis. Due to their potential in cancer treatment there is a broad interest of understanding the biological functions of HATs and HDACs. In this study we focus on HDAC1. It has already been shown that HDACs do not exclusively deacetylate histones but also non-histone proteins (Choudhary et al., 2014). Via mass spectrometry analysis our lab has recently revealed that HDAC1 itself is a non-histone target for acetylation in the human tumor cell line HAP1 (Hess, Moos et al, 2022). It has been shown that K412 was hyperacetylated in HDAC1 WT cells upon treatment with the class I HDAC inhibitor MS275. The same effect can be seen in the HDAC1 CI mutant in which HDAC1 is catalytically inactive but structurally intact. In this mutant K412 was even more hyperacetylated (Figure 5). The HDAC inhibitor MS275 is a class I inhibitor which can inhibit HDAC1, HDAC2 and HDAC3. Interestingly, treatment of HDAC1 CI mutant with the same HDAC inhibitor shows no additional increase on the acetylation of K412 (Figure 5). These data would suggest that HDAC1 is mainly responsible for the deacetylation of K412 (Vcelkova, Simonovic). Proposing autodeacetylation of HDAC1 as a potential mechanism, aroused our interest in deciphering the role of K412ac on HDAC1 function in HAP1 cells. Therefore several HAP1 cell lines expressing different acetyl HDAC1 isoforms (generated in the Master Thesis project of Natalija Cvetcovic) were analyzed. First, we were interested in finding a biological function corresponding to the HDAC1 isoforms with lysine mutations preventing (HDAC1 K412R) or mimicking (HDAC1 K412Q) acetylation of lysine residue K412. Measuring HDAC1 activity of 412R and 412Q mutants using ^{3}H-acetate labeled chicken erythrocyte histones showed no difference in activity between the two acetyl mutants (Figure 7). In another assay we measured HDAC1 stability in the HDAC1 K412R and HDAC1 K412Q mutants via cycloheximide time course experiment. However, the results we obtained (Figure 8) suggest that mimicking or preventing acetylation of K412 doesn't affect the stability of the protein when compared to HDAC1 WT. Taken together, neither activity nor protein stability were in any way effected by mutating the 412R locus into arginine (412R) or glutamine (412Q).

To perform its deacetylase activity HDAC1 needs to be incorporated into co-repressor complexes. Together with HDAC2 it is part of multiprotein complexes such as SIN3A, NuRD and CoREST (Grace et al., 2018). Therefore we wanted to investigate if acetylation of K412 on HDAC1 has an effect on the assembly of HDAC1 with its co-repressor complexes. To examine the interactome of HDAC1 we performed several different assays. First, we immunoprecipitated comparable amounts of FLAG-HDAC1 protein from each isoform and analyzed the samples via Western Blot (Figure 9 A). The binding affinity of HDAC1 to the co-repressor complexes was measured using the corresponding antibodies. In the HDAC1 K412Q mutant, we couldn't show an alteration within the interaction of HDAC1 with the co-repressor complexes SIN3A, NuRD or CoREST in comparison to HDAC1 WT. However, according to the FLAG-IP, the interaction of HDAC1 with its co-repressor complexes seems to be reduced in the HDAC1 K412R mutant, especially concerning SIN3A and HDAC2 (Figure 9B). Since these findings suggest that our target lysine residue 412, in a deacetylated state, negatively affects the binding affinity of HDAC1 to SIN3A and HDAC2, we were determined to reproduce these findings with other interactome studies. Therefore we additionally investigated the interactome of HDAC1 via mass spectrometry analysis. To prevent potential unspecific effects caused by cytosolic proteins in the mass spectrometry approach, we first enriched for nuclear protein via the high salt extraction method (Figure 10). We were curious whether catalytic inactivity and the resulting hyperacetylation of K412 in the HDAC1 CI mutant have an effect on the interactome of HDAC1. Therefore, we additionally used the HDAC1 CI mutant in this experimental setup. The analysis of these interactomes (HDAC1 CI and HDAC1 CI K412R) will be the focus of future studies. Surprisingly, according to the principal component analysis (Figure 11) K412Q mutation showed a similar effect as K412R suggesting that in the case of HDAC1 K412 the mutation to glutamine does not mimic acetylation but, just like arginine, prevents acetylation.

Taking a closer look into the data of the mass spectrometry analysis it can be seen that several proteins exhibit a greater affinity to HDAC1 protein from HDAC1 WT cells when compared to HDAC1 protein from HAP WT cells (Figure 12, panel A). Some of those proteins are known to be interaction partners of the corepressor complexes NURD, SIN3A and CoREST. For example the proteins MBD2, MBD3, GATAD2A, CHD4, MTA1 and MTA3 are part of the NURD deacetylase complex (Brackertz et al., 2006; Helen Hoffmeister et al., 2017). Other proteins that are upregulated in HDAC1 WT when compared to HAP WT are part of the SIN3A deacetylase complex, such as BRMS1, BRMS1L, SAP130, SAP30L, FOXK2, SIN3B and FAM60A (Hurst & Welch, 2011; Fleischer et al., 2003; M Muñoz et al., 2012). Proteins belonging to the CoREST complex such as HMG20B, RCOR2 and RCOR3 were also upregulated in the HDAC1 WT interactome (S Rivero et al., 2015; Ji-hua Xue et al., 2011). Regarding K412R mutation, the interactome is hardly affected (Figure 12, panel D). Most of

the proteins upregulated due to K412R mutation are not known to be part of the co-repressor complexes of HDAC1 and don't play a role in protein acetylation. Only one protein, PHF20, is known to be involved in acetylation. The protein recruits the MOF histone acetyltransferase complex which is involved in acetylation of nucleosomal histone H4 on several lysine residues (Zhang et al., 2016). The data from the FLAG immunoprecipitation experiments indicate a reduced interaction of HDAC1 with SIN3A and HDAC2 in the K412R mutant (Figure 9), for SIN3A this cannot be proven by the data obtained from the mass spectrometry analysis. But the data also show a trend to reduced interaction of HDAC2 with the K412R mutant in comparison to HDAC1 WT (Figure 12). Most of the proteins that are only part of the K412R interactome are involved in DNA repair (Figure 12, panel D). Namely PARP1/2, LIG3, XRCC1 and APTX. BCL11B protein is known to be a transcriptional repressor, and is regulated by the NURD nucleosome remodeling and histone deacetylase complex (Cismasiu et al., 2008). KANSL 1/2 is also involved in histone acetylation. As part of the NSL complex it is involved in acetylation of nucleosomal histone H4 on several lysine residues and therefore may be involved in the regulation of transcription (Dias et al., 2014). In the same experimental approach we compared the interactome of the HDAC1 CI mutant with the HDAC1 CI K412R mutant, in both HDAC1 is catalytically inactive and only differs in its lysine 412 which is resistant to acetylation in the HDAC1 CI K412R mutant. Proteins that are only part of the HDAC1 CI K412R interactome include NCOR2, BCL11B, JADE3, ANKRD11 and DBNL. NCOR2 is a transcriptional silencer and acts as a multisubunit complex which includes histone deacetylases (Jones & Shi, 2003). BCL11B also appeared in the K412R interactome and is regulated by the NURD nucleosome remodeling and histone deacetylase complex. There are no other proteins affected which are part of any of the multisubunit complexes which interact with HDAC1/2. These results suggest, that the acetylation state of lysine 412 on HDAC1 doesn't have a big impact on the ability of HDAC1 to interact with its common co-repressor complexes or to perform its deacetylase activity. However, FLAG immunoprecipitation experiments indicate reduced binding of HDAC1 to SIN3A and HDAC2.

Therefore, we investigated the behavior of HDAC2 and SIN3A in the K412R mutant in more detail, performing HDAC2 and SIN3A co-immunoprecipitation experiments. Regarding the signal of HDAC1 in the Western blot analysis, we obtained a much stronger signal in HDAC1 WT then in the HDAC1 K412R mutant although the same amount of HDAC2 protein was precipitated (Figure 13). This again indicates that HDAC1 interacts less with HDAC2 in the K412R acetyl mutant. Part of the HDAC2 immunoprecipitate was also used to measure HDAC activity, but no significant difference between the K412R mutant and HDAC1 WT was detected (Figure 14B). Although, Western blot analysis suggests a reduced interaction of HDAC1 with HDAC2 in the K412R mutant it doesn't seem to affect the deacetylase activity associated with HDAC1.

A preliminary Western blot analysis of proteins co-precipitated with SIN3A showed a stronger signal for HDAC1 and HDAC2 in the K412R mutant compared to HDAC1 WT (Figure 15). This result must be validated, since it is contrary to the Western blot analysis of precipitated FLAG-HDAC1 which showed a weaker signal of HDAC1 in the K412R mutant compared to HDAC1 WT (Figure 9). Again, part of the immunoprecipitated SIN3A protein was used to measure HDAC activity. The data obtained from the activity assay showed no difference in deacetylase activity of HDAC1 in the K412R mutant compared to HDAC1 WT (Figure 16).
In summary, one can say that lysine 412 being resistant to acetylation does not prevent HDAC1 to perform its deacetylase activity. Concerning, the interactome of HDAC1 in the K412R mutant, both, FLAG-IP and HDAC2 co IP, suggest a reduced interaction of HDAC1 with HDAC2 upon lysine 412 mutation. For SIN3A we cannot say for sure if its interaction with HDAC1 is affected in the acetylation resistant mutant, since FLAG IP and SIN3A IP yield differently. With these first two parts of the study, we aimed to characterize the HAP1 cell lines expressing acetyl HDAC1 mutant regarding their deacetylase activity, protein stability and interaction with other proteins. Throughout the study we especially focused on the HDAC1 K412R mutant, in which lysine 412 on HDAC1 is resistant to acetylation, compared to HDAC1 WT. Summarizing all biochemical assays we performed, it strikes that predominantly the interaction of HDAC1 with HDAC2 seems to be affected upon the mutation on lysine 412. Future studies will address additional roles of acetylated lysine 412 on HDAC1.

Another goal of this study, was to characterize an antibody that specifically recognizes acetylated K412 on HDAC1. The aim was to make the antibody applicable for experiments such as immunoprecipitation, Western blot analysis and FACS analysis. During my Master thesis I generated tools and developed methods to identify acetyl-K412 specific antibodies in mouse sera and polyclonal and monoclonal cell supernatants. In our experimental approach the HDAC CI mutant was used as positive control. Since HDAC1 CI is catalytically inactive and the protein itself is hyperacetylated on lysine residue 412, we expected a strong signal when incubated with the antibody. HDAC1 CI K412R was employed as negative control. Here, K412 is resistant to acetylation and should not be recognized by our specific antibody.
The first serum screens were performed on whole cell extracts of the two mutants. In this case we weren't able to see any signals (Figure 18), most probably because only a very small fraction of HDAC1 is present in an acetylated state. To better detect acetylated proteins with the mouse sera we enriched for acetylated proteins performing acetyl-lysine immunoprecipitation (Figure 19). When running the serum screen on the acetyl immunoprecipitates we were finally able to detect a signal at the height of HDAC1 in the HDAC1 CI mutant but not in the HDAC1 CI K412R mutant (Figure 20). Based on these findings the two most promising mice were sacrificed and single clones were prepared which should produce our desired antibody.

However, when screening the monoclonal supernatant 8D7-E4 on the acetyl immunoprecipitates, a signal in both mutants emerged. This indicates that the antibody present in the supernatant is not specific for acetylated lysine 412 on HDAC1 but also recognizes K412 on HDAC1 in a deacetylated state (HDAC1 CI K412R mutant) (Figure 21B). Due to these findings we decided to repeat the single cell dilution with another polyclonal cell mixture (5G12). With this new polyclonal supernatant, we repeated the screen on the acetyl immunoprecipitates and eventually were able to show the specificity of the antibody present in the supernatant (Figure 23). The Western blot analysis only displayed a signal in the HDAC1 CI mutant when incubated with the mixed clone 5G12 but not in the HDAC1 CI K412R mutant indicating that the antibody present in this new supernatant only recognizes acetylated K412 on HDAC1.

In a further step we performed a single cell dilution with 5G12 and obtained the new monoclonal supernatant (5G12-3H3-D8). As Figure 24 reveals, the antibody present in the monoclonal supernatant, is able to recognize acetylated lysine 412 on FLAG-immunoprecipitated HDAC1, even when not enriched for acetylated proteins. The yet produced antibody shows specificity towards acetylated lysine 412 on HDAC1 and is sensitive enough to detect acetylated protein even if not especially enriched for acetylated proteins.

Taken together we succeeded in the generation of a monoclonal mouse antibody that recognizes HDAC1 CI protein by Western blot analysis of FLAG immunoprecipitates. In future studies, it will be interesting to investigate whether the antibody recognizes also less acetylated wildtype protein and is functional in indirect immunofluorescence experiments and FACS analysis. Finally, the monoclonal antibody can be tested in immunoprecipitation experiments to identify interactors which specifically bind to K412 acetylated HDAC1.

5. References

Arents G, Burlingame RW, Wang BC, Love WE, Moudrianakis EN. The nucleosomal core histone octamer at 3.1 A resolution: a tripartite protein assembly and a left-handed superhelix. Proc Natl Acad Sci U S A. 1991 Nov 15;88(22):10148-52. doi: 10.1073/pnas.88.22.10148. PMID: 1946434; PMCID: PMC52885.

Bannister, A., Kouzarides, T. Regulation of chromatin by histone modifications. Cell Res 21, 381–395 (2011). https://doi.org/10.1038/cr.2011.22

Biterge B. A mini review on post-translational histone modifications. MOJ Cell Sci Rep. 2016;3(1):26-28. DOI: 10.15406/mojcsr.2016.03.00047

Botrugno OA, Robert T, Vanoli F, Foiani M, Minucci S. Molecular pathways: old drugs define new pathways: non-histone acetylation at the crossroads of the DNA damage response and autophagy. Clin Cancer Res. 2012 May 1;18(9):2436-42. doi: 10.1158/1078-0432.CCR-11-0767. Epub 2012 Apr 18. PMID: 22512979.

Bowman GD, Poirier MG. Post-translational modifications of histones that influence nucleosome dynamics. Chem Rev. 2015 Mar 25;115(6):2274-95. doi: 10.1021/cr500350x. Epub 2014 Nov 26. PMID: 25424540; PMCID: PMC4375056.

Brackertz M, Gong Z, Leers J, Renkawitz R. p66alpha and p66beta of the Mi-2/NuRD complex mediate MBD2 and histone interaction. Nucleic Acids Res. 2006 Jan 13;34(2):397-406. doi: 10.1093/nar/gkj437. PMID: 16415179; PMCID: PMC1331983.

Brunmeir, Reinhard & Lagger, Sabine & Seiser, Christian. (2009). Histone deacetylase HDAC1/HDAC2-controlled embryo development and cell differentiation. The International journal of developmental biology. 53. 275-89. 10.1387/ijdb.082649rb.

Caiafa P, Zampieri M. DNA methylation and chromatin structure: the puzzling CpG islands. J Cell Biochem. 2005 Feb 1;94(2):257-65. doi: 10.1002/jcb.20325. PMID: 15546139.

Chen Y, Yang Y, Wang F, Wan K, Yamane K, Zhang Y, Lei M. Crystal structure of human histone lysine-specific demethylase 1 (LSD1). Proc Natl Acad Sci U S A. 2006 Sep 19;103(38):13956-61. doi: 10.1073/pnas.0606381103. Epub 2006 Sep 6. PMID: 16956976; PMCID: PMC1599895.

Chen, Z., Zhang, Y. Maternal H3K27me3-dependent autosomal and X chromosome imprinting. Nat Rev Genet 21, 555–571 (2020). https://doi.org/10.1038/s41576-020-0245-9

Choudhary C, Kumar C, Gnad F, Nielsen ML, Rehman M, Walther TC, Olsen JV, Mann M. Lysine acetylation targets protein complexes and co-regulates major cellular functions.

Science. 2009 Aug 14;325(5942):834-40. doi: 10.1126/science.1175371. Epub 2009 Jul 16. PMID: 19608861.

Choudhary, C., Weinert, B., Nishida, Y. et al. The growing landscape of lysine acetylation links metabolism and cell signalling. Nat Rev Mol Cell Biol 15, 536–550 (2014). https://doi.org/10.1038/nrm3841

Cismasiu VB, Paskaleva E, Suman Daya S, Canki M, Duus K, Avram D. BCL11B is a general transcriptional repressor of the HIV-1 long terminal repeat in T lymphocytes through recruitment of the NuRD complex. Virology. 2008 Oct 25;380(2):173-81. doi: 10.1016/j.virol.2008.07.035. Epub 2008 Sep 2. PMID: 18768194; PMCID: PMC2637995.

Clapier CR, Cairns BR. The biology of chromatin remodeling complexes. Annu Rev Biochem. 2009;78:273-304. doi: 10.1146/annurev.biochem.77.062706.153223. PMID: 19355820.

Cremer T, Cremer M. Chromosome territories. Cold Spring Harb Perspect Biol. 2010 Mar;2(3):a003889. doi: 10.1101/cshperspect.a003889. PMID: 20300217; PMCID: PMC2829961.

Dias J, Van Nguyen N, Georgiev P, Gaub A, Brettschneider J, Cusack S, Kadlec J, Akhtar A. Structural analysis of the KANSL1/WDR5/KANSL2 complex reveals that WDR5 is required for efficient assembly and chromatin targeting of the NSL complex. Genes Dev. 2014 May 1;28(9):929-42. doi: 10.1101/gad.240200.114. PMID: 24788516; PMCID: PMC4018492.

Egger, G., Liang, G., Aparicio, A. et al. Epigenetics in human disease and prospects for epigenetic therapy. Nature 429, 457–463 (2004). https://doi.org/10.1038/nature02625

Elena Battaglioli, Maria E. Andrés, Dave W. Rose, Josh G. Chenoweth, Michael G. Rosenfeld, Mary E. Anderson, Gail Mandel, REST Repression of Neuronal Genes Requires Components of the hSWI·SNF Complex*, Journal of Biological Chemistry, Volume 277, Issue 43, 2002, Pages 41038-41045, ISSN 0021-9258, https://doi.org/10.1074/jbc.M205691200.

Ellmeier W, Seiser C. Histone deacetylase function in CD4+ T cells. Nat Rev Immunol. 2018 Oct;18(10):617-634. doi: 10.1038/s41577-018-0037-z. Erratum in: Nat Rev Immunol. 2019 Apr;19(4):266. PMID: 30022149.

Fleischer TC, Yun UJ, Ayer DE. Identification and characterization of three new components of the mSin3A corepressor complex. Mol Cell Biol. 2003 May;23(10):3456-67. doi: 10.1128/MCB.23.10.3456-3467.2003. PMID: 12724404; PMCID: PMC164750.

Gibney, E., Nolan, C. Epigenetics and gene expression. Heredity 105, 4–13 (2010). https://doi.org/10.1038/hdy.2010.54

Gillette TG, Hill JA. Readers, writers, and erasers: chromatin as the whiteboard of heart disease. Circ Res. 2015 Mar 27;116(7):1245-53. doi: 10.1161/CIRCRESAHA.116.303630. PMID: 25814685; PMCID: PMC4380191.

Glozak MA, Sengupta N, Zhang X, Seto E. Acetylation and deacetylation of non-histone proteins. Gene. 2005 Dec 19;363:15-23. doi: 10.1016/j.gene.2005.09.010. Epub 2005 Nov 11. PMID: 16289629.

Grace E. Adams, Aditya Chandru, Shaun M. Cowley; Co-repressor, co-activator and general transcription factor: the many faces of the Sin3 histone deacetylase (HDAC) complex. Biochem J 21 December 2018; 475 (24): 3921–3932. doi: https://doi.org/10.1042/BCJ20170314

Gu W, Roeder RG. Activation of p53 sequence-specific DNA binding by acetylation of the p53 C-terminal domain. Cell. 1997 Aug 22;90(4):595-606. doi: 10.1016/s0092-8674(00)80521-8. PMID: 9288740.

Hansen, B.K., Gupta, R., Baldus, L. et al. Analysis of human acetylation stoichiometry defines mechanistic constraints on protein regulation. Nat Commun 10, 1055 (2019). https://doi.org/10.1038/s41467-019-09024-0

Harald Khier, Stefan Bartl, Bernd Schuettengruber, Christian Seiser, Molecular cloning and characterization of the mouse histone deacetylase 1 gene: integration of a retrovirus in 129SV mice, Biochimica et Biophysica Acta (BBA) - Gene Structure and Expression, Volume 1489, Issues 2–3, 1999, Pages 365-373, ISSN 0167-4781, https://doi.org/10.1016/S0167-4781(99)00203-1. (https://www.sciencedirect.com/science/article/pii/S0167478199002031)

Helen Hoffmeister, Andreas Fuchs, Fabian Erdel, Sophia Pinz, Regina Gröbner-Ferreira, Astrid Bruckmann, Rainer Deutzmann, Uwe Schwartz, Rodrigo Maldonado, Claudia Huber, Anne-Sarah Dendorfer, Karsten Rippe, Gernot Längst, CHD3 and CHD4 form distinct NuRD complexes with different yet overlapping functionality, Nucleic Acids Research, Volume 45, Issue 18, 13 October 2017, Pages 10534–10554, https://doi.org/10.1093/nar/gkx711

Hess L, Moos V, Lauber AA, Reiter W, Schuster M, Hartl N, Lackner D, Boenke T, Koren A, Guzzardo PM, Gundacker B, Riegler A, Vician P, Miccolo C, Leiter S, Chandrasekharan MB, Vcelkova T, Tanzer A, Jun JQ, Bradner J, Brosch G, Hartl M, Bock C, Bürckstümmer T, Kubicek S, Chiocca S, Bhaskara S, Seiser C. A toolbox for class I HDACs reveals isoform specific roles in gene regulation and protein acetylation. PLoS Genet. 2022 Aug 22;18(8):e1010376. doi: 10.1371/journal.pgen.1010376. PMID: 35994477; PMCID: PMC9436093.

Hurst DR, Welch DR. Unraveling the enigmatic complexities of BRMS1-mediated metastasis suppression. FEBS Lett. 2011 Oct 20;585(20):3185-90. doi: 10.1016/j.febslet.2011.07.045. Epub 2011 Aug 5. PMID: 21827753; PMCID: PMC3195837.

Jaenisch R, Bird A. Epigenetic regulation of gene expression: how the genome integrates intrinsic and environmental signals. Nat Genet. 2003 Mar;33 Suppl:245-54. doi: 10.1038/ng1089. PMID: 12610534.

Jenuwein T, Allis CD. Translating the histone code. Science. 2001 Aug 10;293(5532):1074-80. doi: 10.1126/science.1063127. PMID: 11498575.

Jones PL, Shi YB. N-CoR-HDAC corepressor complexes: roles in transcriptional regulation by nuclear hormone receptors. Curr Top Microbiol Immunol. 2003;274:237-68. doi: 10.1007/978-3-642-55747-7_9. PMID: 12596910.

Karki, 2020 Cell Biology, Genetics https://www.onlinebiologynotes.com/chromatin-structure-composition-and-packaging/

Kim HJ, Bae SC. Histone deacetylase inhibitors: molecular mechanisms of action and clinical trials as anti-cancer drugs. Am J Transl Res. 2011 Feb;3(2):166-79. Epub 2010 Dec 26. PMID: 21416059; PMCID: PMC3056563.

Kong Y, Jung M, Wang K, Grindrod S, Velena A, Lee SA, Dakshanamurthy S, Yang Y, Miessau M, Zheng C, Dritschilo A, Brown ML. Histone deacetylase cytoplasmic trapping by a novel fluorescent HDAC inhibitor. Mol Cancer Ther. 2011 Sep;10(9):1591-9. doi: 10.1158/1535-7163.MCT-10-0779. Epub 2011 Jun 22. PMID: 21697394; PMCID: PMC3695633.

Laherty CD, Yang WM, Sun JM, Davie JR, Seto E, Eisenman RN. Histone deacetylases associated with the mSin3 corepressor mediate mad transcriptional repression. Cell. 1997 May 2;89(3):349-56. doi: 10.1016/s0092-8674(00)80215-9. PMID: 9150134.

Li E, Zhang Y. DNA methylation in mammals. Cold Spring Harb Perspect Biol. 2014 May 1;6(5):a019133. doi: 10.1101/cshperspect.a019133. PMID: 24789823; PMCID: PMC3996472.

Li Z, Zhu WG. Targeting histone deacetylases for cancer therapy: from molecular mechanisms to clinical implications. Int J Biol Sci. 2014 Jul 2;10(7):757-70. doi: 10.7150/ijbs.9067. PMID: 25013383; PMCID: PMC4081609.

Loredana Verdone, Eleonora Agricola, Micaela Caserta, Ernesto Di Mauro, Histone acetylation in gene regulation, Briefings in Functional Genomics, Volume 5, Issue 3, September 2006, Pages 209–221, https://doi.org/10.1093/bfgp/ell028

Luger, K., Mäder, A., Richmond, R. et al. Crystal structure of the nucleosome core particle at 2.8 Å resolution. Nature 389, 251–260 (1997). https://doi.org/10.1038/38444

Marmorstein R, Zhou MM. Writers and readers of histone acetylation: structure, mechanism, and inhibition. Cold Spring Harb Perspect Biol. 2014 Jul 1;6(7):a018762. doi: 10.1101/cshperspect.a018762. PMID: 24984779; PMCID: PMC4067988.

Marzluff WF Jr, McCarty KS. Two classes of histone acetylation in developing mouse mammary gland. J Biol Chem. 1970 Nov 10;245(21):5635-42. PMID: 5472362.

Millard CJ, Watson PJ, Celardo I, Gordiyenko Y, Cowley SM, Robinson CV, Fairall L, Schwabe JW. Class I HDACs share a common mechanism of regulation by inositol phosphates. Mol Cell. 2013 Jul 11;51(1):57-67. doi: 10.1016/j.molcel.2013.05.020. Epub 2013 Jun 20. PMID: 23791785; PMCID: PMC3710971.

Miller TA, Witter DJ, Belvedere S. Histone deacetylase inhibitors. J Med Chem. 2003 Nov 20;46(24):5097-116. doi: 10.1021/jm0303094. PMID: 14613312.

Moon BS, Yun HM, Chang WH, Steele BH, Cai M, Choi SH, Lu W. Smek promotes corticogenesis through regulating Mbd3's stability and Mbd3/NuRD complex recruitment to genes associated with neurogenesis. PLoS Biol. 2017 May 3;15(5):e2001220. doi: 10.1371/journal.pbio.2001220. PMID: 28467410; PMCID: PMC5414985.

Moris, N., Pina, C. & Arias, A. Transition states and cell fate decisions in epigenetic landscapes. Nat Rev Genet 17, 693–703 (2016). https://doi.org/10.1038/nrg.2016.98

Moser MA, Hagelkruys A, Seiser C. Transcription and beyond: the role of mammalian class I lysine deacetylases. Chromosoma. 2014 Mar;123(1-2):67-78. doi: 10.1007/s00412-013-0441-x. Epub 2013 Oct 30. PMID: 24170248; PMCID: PMC3967066.

Muñoz IM, MacArtney T, Sanchez-Pulido L, Ponting CP, Rocha S, Rouse J. Family with sequence similarity 60A (FAM60A) protein is a cell cycle-fluctuating regulator of the SIN3-HDAC1 histone deacetylase complex. J Biol Chem. 2012 Sep 21;287(39):32346-53. doi: 10.1074/jbc.M112.382499. Epub 2012 Aug 3. PMID: 22865885; PMCID: PMC3463326.

Narita, T., Weinert, B.T. & Choudhary, C. Functions and mechanisms of non-histone protein acetylation. Nat Rev Mol Cell Biol 20, 156–174 (2019). https://doi.org/10.1038/s41580-018-0081-3

Paszkowski J, Whitham SA. Gene silencing and DNA methylation processes. Curr Opin Plant Biol. 2001 Apr;4(2):123-9. doi: 10.1016/s1369-5266(00)00147-3. PMID: 11228434.

Popova EY, Grigoryev SA, Fan Y, Skoultchi AI, Zhang SS, Barnstable CJ. Developmentally regulated linker histone H1c promotes heterochromatin condensation and mediates structural integrity of rod photoreceptors in mouse retina. J Biol Chem. 2013 Jun 14;288(24):17895-907. doi: 10.1074/jbc.M113.452144. Epub 2013 May 3. PMID: 23645681; PMCID: PMC3682587.

Qiu Y, Zhao Y, Becker M, John S, Parekh BS, Huang S, Hendarwanto A, Martinez ED, Chen Y, Lu H, Adkins NL, Stavreva DA, Wiench M, Georgel PT, Schiltz RL, Hager GL. HDAC1 acetylation is linked to progressive modulation of steroid receptor-induced gene transcription. Mol Cell. 2006 Jun 9;22(5):669-79. doi: 10.1016/j.molcel.2006.04.019. PMID: 16762839.

Reed SM, Quelle DE. p53 Acetylation: Regulation and Consequences. Cancers (Basel). 2014 Dec 23;7(1):30-69. doi: 10.3390/cancers7010030. PMID: 25545885; PMCID: PMC4381250.

Rivero S, Ceballos-Chávez M, Bhattacharya SS, Reyes JC. HMG20A is required for SNAI1-mediated epithelial to mesenchymal transition. Oncogene. 2015 Oct 8;34(41):5264-76. doi: 10.1038/onc.2014.446. Epub 2015 Feb 2. PMID: 25639869.

Robertson, K. DNA methylation and human disease. Nat Rev Genet 6, 597–610 (2005). https://doi.org/10.1038/nrg1655

Rossetto D, Avvakumov N, Côté J. Histone phosphorylation: a chromatin modification involved in diverse nuclear events. Epigenetics. 2012 Oct;7(10):1098-108. doi: 10.4161/epi.21975. Epub 2012 Sep 4. PMID: 22948226; PMCID: PMC3469451.

Singh BN, Zhang G, Hwa YL, Li J, Dowdy SC, Jiang SW. Nonhistone protein acetylation as cancer therapy targets. Expert Rev Anticancer Ther. 2010 Jun;10(6):935-54. doi: 10.1586/era.10.62. PMID: 20553216; PMCID: PMC3273412.

Sung Chan Kim, Robert Sprung, Yue Chen, Yingda Xu, Haydn Ball, Jimin Pei, Tzuling Cheng, Yoonjung Kho, Hao Xiao, Lin Xiao, Nick V. Grishin, Michael White, Xiang-Jiao Yang, Yingming Zhao, Substrate and Functional Diversity of Lysine Acetylation Revealed by a Proteomics Survey, Molecular Cell, Volume 23, Issue 4, 2006, Pages 607-618, ISSN 1097-2765, https://doi.org/10.1016/j.molcel.2006.06.026. (https://www.sciencedirect.com/science/article/pii/S1097276506004540)

Suraweera A, O'Byrne KJ, Richard DJ. Combination Therapy With Histone Deacetylase Inhibitors (HDACi) for the Treatment of Cancer: Achieving the Full Therapeutic Potential of HDACi. Front Oncol. 2018 Mar 29;8:92. doi: 10.3389/fonc.2018.00092. PMID: 29651407; PMCID: PMC5884928.

Tamaru H. Confining euchromatin/heterochromatin territory: jumonji crosses the line. Genes Dev. 2010 Jul 15;24(14):1465-78. doi: 10.1101/gad.1941010. PMID: 20634313; PMCID: PMC2904936.

Thiagalingam S, Cheng KH, Lee HJ, Mineva N, Thiagalingam A, Ponte JF. Histone deacetylases: unique players in shaping the epigenetic histone code. Ann N Y Acad Sci. 2003 Mar;983:84-100. doi: 10.1111/j.1749-6632.2003.tb05964.x. PMID: 12724214.

Thompson PR, Wang D, Wang L, Fulco M, Pediconi N, Zhang D, An W, Ge Q, Roeder RG, Wong J, Levrero M, Sartorelli V, Cotter RJ, Cole PA. Regulation of the p300 HAT domain via a novel activation loop. Nat Struct Mol Biol. 2004 Apr;11(4):308-15. doi: 10.1038/nsmb740. Epub 2004 Mar 7. PMID: 15004546.

Timmermann, S., Lehrmann, H., Polesskaya, A. et al. Histone acetylation and disease. CMLS, Cell. Mol. Life Sci. 58, 728–736 (2001). https://doi.org/10.1007/PL00000896

Turner BM. Histone acetylation and control of gene expression. J Cell Sci. 1991 May;99 (Pt 1):13-20. doi: 10.1242/jcs.99.1.13. PMID: 1757496.

Vaquero, A., Sternglanz, R. & Reinberg, D. NAD+-dependent deacetylation of H4 lysine 16 by class III HDACs. Oncogene 26, 5505–5520 (2007). https://doi.org/10.1038/sj.onc.1210617

Voelter-Mahlknecht S, Ho AD, Mahlknecht U. Chromosomal organization and localization of the novel class IV human histone deacetylase 11 gene. Int J Mol Med. 2005 Oct;16(4):589-98. PMID: 16142391.

Waterland RA. Epigenetic mechanisms and gastrointestinal development. J Pediatr. 2006 Nov; 149 (5 Suppl): S137-42. doi: 10.1016/j.jpeds.2006.06.064. PMID: 17212956.

Wilkinson KA, Henley JM. Mechanisms, regulation and consequences of protein SUMOylation. Biochem J. 2010 May 13;428(2):133-45. doi: 10.1042/BJ20100158. PMID: 20462400; PMCID: PMC3310159.

Winter M, Moser MA, Meunier D, Fischer C, Machat G, Mattes K, Lichtenberger BM, Brunmeir R, Weissmann S, Murko C, Humer C, Meischel T, Brosch G, Matthias P, Sibilia M, Seiser C. Divergent roles of HDAC1 and HDAC2 in the regulation of epidermal development and tumorigenesis. EMBO J. 2013 Dec 11;32(24):3176-91. doi: 10.1038/emboj.2013.243. Epub 2013 Nov 15. PMID: 24240174; PMCID: PMC3981143.

Xue JH, Zheng M, Xu XW, Wu SS, Chen Z, Chen F. Involvement of REST corepressor 3 in prognosis of human hepatitis B. Acta Pharmacol Sin. 2011 Aug;32(8):1019-24. doi: 10.1038/aps.2011.49. Epub 2011 Jul 18. PMID: 21765449; PMCID: PMC4002525.

Zhang Y, Ng HH, Erdjument-Bromage H, Tempst P, Bird A, Reinberg D. Analysis of the NuRD subunits reveals a histone deacetylase core complex and a connection with DNA methylation. Genes Dev. 1999 Aug 1;13(15):1924-35. doi: 10.1101/gad.13.15.1924. PMID: 10444591; PMCID: PMC316920.

Zhang, X., Peng, D., Xi, Y. et al. G9a -mediated methylation of ERα links the PHF20/MOF histone acetyltransferase complex to hormonal gene expression. Nat Commun 7, 10810 (2016). https://doi.org/10.1038/ncomms10810

Zhibin Wang, Chongzhi Zang, Kairong Cui, Dustin E. Schones, Artem Barski, Weiqun Peng, Keji Zhao, Genome-wide Mapping of HATs and HDACs Reveals Distinct Functions in Active and Inactive Genes, Cell, Volume 138, Issue 5, 2009, Pages 1019-1031, ISSN 0092-8674, https://doi.org/10.1016/j.cell.2009.06.049.